MASTER THESIS 2012

The influence of salt in the formation of carboxylic functionalized mesoporous silica

LUND UNIVERSITY

Master program of Organizing Molecular Matter

Author: Ruiyu Lin

Supervisor: Prof. Viveka Alfredsson

To be presented for public defence on May 4th 2012 at the department of Physical Chemistry, Kemicentrum, Lund University.

Abstract

Carboxylic group functionalized mesoporous silicas (CFMSs) were synthesized using cationic Gemini surfactant ($C_{18\text{-}3\text{-}1}$) as structure director and an anionic co-structure directing agents (CSDA). Well ordered mixture of CCP ($Fm\bar{3}m$) and HCP ($P6_3/mmc$), and cubic $Fd\bar{3}m$ structures were obtained. Non-uniform morphologies were observed.

This thesis has been focused on the salt influence on the formation of CFMS materials and how the material properties are affected. Monovalent NaCl and divalent $CaCl_2$ have been added to the syntheses.

The structure, the morphology and the particle size of the CFMSs were investigated with small angle x-ray diffraction (SAXD) and scanning electronic microscopy (SEM). Addition of salt influenced the structure transformation within a limited pH range. Further the morphology and the particle size was influenced in the entire pH-range investigated. Moreover, well defined morphologies are more easily obtained with a high salt concentration. The influence of NaCl and $CaCl_2$ showed qualitative similar but quantitative different results.

Popular Scientific Summary

This master thesis was focused on the influence of salt, such as NaCl and $CaCl_2$, in the formation of carboxylic functionalized mesoporous silica materials.

Mesoporous silica materials are one type of porous materials with a pore size between 2 and 5 nm ($1nm = 0.000000001\ m$). The walls of the pores in this kind of materials consist of silicon dioxide, which is called silica (sand). The mesoporous silica materials, or rather the mesoporous silica particles, are formed by amphiphilic molecules, a kind of molecule with one part that loves water and one part that hates water, and a silica source. Within the group of amphiphilic molecules, surfactants are mostly used. The surfactants are molecules with positive or negative charged head groups, which love water, and long organic tails, that hate water. Examples of surfactants in our daily life are shampoo and detergent. When the surfactants have been dissolved in water, the tails that hate water will get together and only leave the charged head groups outside in contact with the water. In this case, the grouped surfactants can form different shapes with the tails inside and the head groups on the surface of the shapes. The silica source will build up walls around these shapes. Accordingly, the "mesopores" of the materials are filled with surfactants during their creation. When the surfactants are removed, the mesopores arise, and the mesoporous materials with silica walls are formed. The networks of mesopores are often well ordered in various structures. When adding acid or salt into the formation mixture of mesoporous silica materials, the structure or the shape of the materials (particles) can sometimes be changed. The process is like baking, when adding different things, such as baking powder or salt, the shape or the texture of the pastries can be changed.

In the work of this thesis, a surfactant with positive charged head group was used. Moreover, one kind of molecule consists of a negative part and a silicon part was added in the mixture. The negative part of this molecule is called carboxylic group, which is the major component of vinegar. In the mixture, this molecule will be in contact with the surfactant head group via the carboxylic part and in contact with the silica source via the silicon part. After the formation, when the surfactants are removed, the carboxylic groups will remain within the pores, therefore, carboxylic functionalized mesoporous silica (CFMS) materials are formed. Addition of acid can change the structures of the CFMS materials. The shapes of the particles can change depending on the structure. In this work we show that addition of salt can change the structures and the shapes of the CFMS particles. Additionally, the particle sizes increase when the amount of salt increases. Some of the CFMS particles have interesting and well-defined shapes, as shown in Figure 1. This means that salts can be used as control chemicals in the formation.

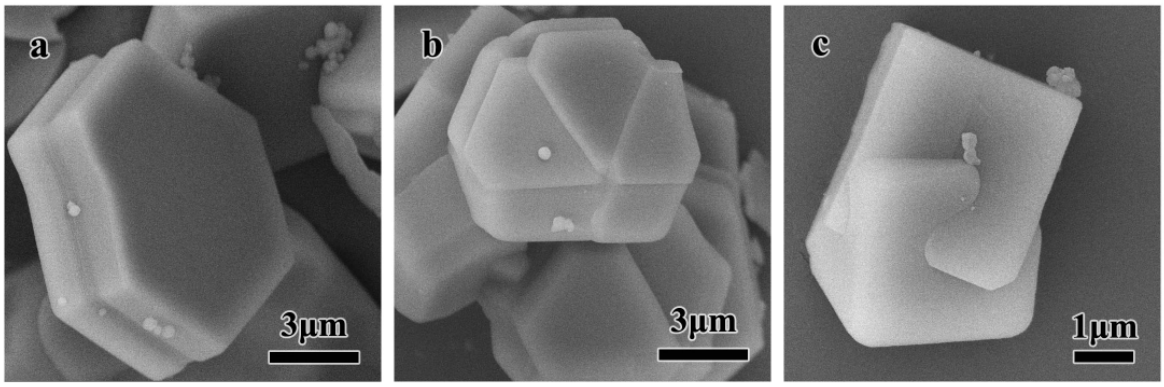

Figure 1, Scanning electron microscopy images of the CFMS particles with well defined shapes. a), hexagonal plate; b), "flower" like shape; c), cube like shape. ($1\mu m = 0.000001\ m$)

List of Abbreviations

1D	one-dimensional
2D	two-dimensional
3D	three dimensional
AMS	anionic surfactant templated mesoporous silica
APS	3-aminopropyltrimethoxysilane
$C_{18\text{-}3\text{-}1}$	gemini surfactant $[C_{18}H_{37}N(CH_3)_3N(CH_3)_3]Br_2$
CCP	cubic close-packed
CES	carboxyethylsilanetriol sodium salt
CFMSs	carboxylic group functionalized mesoporous silicas
CMC	critical micellar concentration
CSDA	co-structure direction agent
CTAB	cetyltrimethyl-ammnonium bromide
HCP	hexagonal close-packed
IUPAC	International Union of Pure and Applied Chemistry
MCM-41	2-dimensional hexagonal (*p*6*mm*) silica formed with cationic surfactants, first synthesized by the Mobil group
MCM-48	bi-continuous cubic mesostructured (*Ia*3*d*) silica formed with cationic surfactants, first synthesized by the Mobil group
MCM-50	lamellar structured silica formed with cationic surfactants, first synthesized by the Mobil group
PEO	polyethylene oxide
PPO	polypropylene oxide
SAXD	small angle x-ray diffraction
SAXS	small angle x-ray scattering
SBA	Santa Barbara Amorphous
SBA-12	3-dimensional hexagonal (*P6*$_3$/*mmc*) silica formed with Pluronics, first synthesized by the group in Santa Barbara

SBA-15	2-dimensional hexagonal (*p*6*mm*) silica formed with Pluronics, first synthesized by the group in Santa Barbara
SEM	scanning electron microscope
SMC	silica mesoporous crystal
TCP	tetrahedrally close-packed
TEM	transmission electron microscopy
TEOS	tetraethyl orthosilicate
TMAPS	*N*-trimethoxysilylpropyl-*N*,*N*,*N*-trimethylammonium chloride
XRD	x-ray diffraction

Contents

1. Introduction

The developments of mesoporous silica materials have been interesting for materials science since the early 1990s. Mesoporous silicas can be made in many structural variants and are interesting for applications in fields of catalysis, separation, drug delivery and so on.

Mesoporous silica can be synthesized using different methods. The typical synthesis strategy is to use amphiphiles as a structure director and let the silica source aggregate around the hydrophilic parts of the amphiphilies. In 2003, Che et al suggested a synthesis method introducing a co-structure directing agent (CSDA) in to the synthesis system.[1] Functional mesoporous silica materials with various structures have been synthesized via the CSAD method. Using cationic surfactant as template and anionic CSDA, carboxylic group functionalized mesoporous silicas (CFMSs) were synthesized. Han et al showed that the material change structure as the HCl concentration was varied.[2] They detected a transformation from $Fm\bar{3}m$ to $Fd\bar{3}m$ as the acidity was increased. In this thesis we investigate the influence of salt on the properties of CFMS.

This chapter is aimed to give a brief introduction to the present thesis work, the synthesis, background and characterization of the silica mesoporous crystals.

1.1 Mesoporous materials

Ordered mesoporous materials are materials having an interconnected network of pores with pore size between 2 and 50 nm. This pore size regime, defined by the International Union of Pure and Applied Chemistry (IUPAC),[3] is called meso-. The first materials of this class were synthesized about two decades ago.[4-6] As the materials have high surface area and large pore volume, the materials have attracted considerable interest, based on their potential development and applications in nanotechnology. In the family of mesoporous material, the silica materials can attain most structures.

Structurely, mesoporous materials are analogous to lyotropic liquid crystal systems. This implies that the surfactants form mesoscopic phases, depending on their concentration and temperature. As shown in Figure 1.1 (a phase diagram above the Kraft temperature in a lyotropic system) micellar, cubic, columnar, bi-continuous and lamellar phases are formed at different surfactant concentrations. Compared to the liquid crystal system, ordered mesoporous silica has a skeletal wall made up of amorphous silica instead of water. The “mesopores” are filled with surfactants during synthesis. It is only after removing the surfactant that the porous structure arises. The

networks of pores are often arranged in ordered one-dimensional (1D), two-dimensional (2D) or three-dimensional (3D) topological structures. The ordered mesoporous silica can also be regarded as a "cavity crystal" on the mesoscale. The acronym SMC will from now on be used for silica mesoporous crystal.

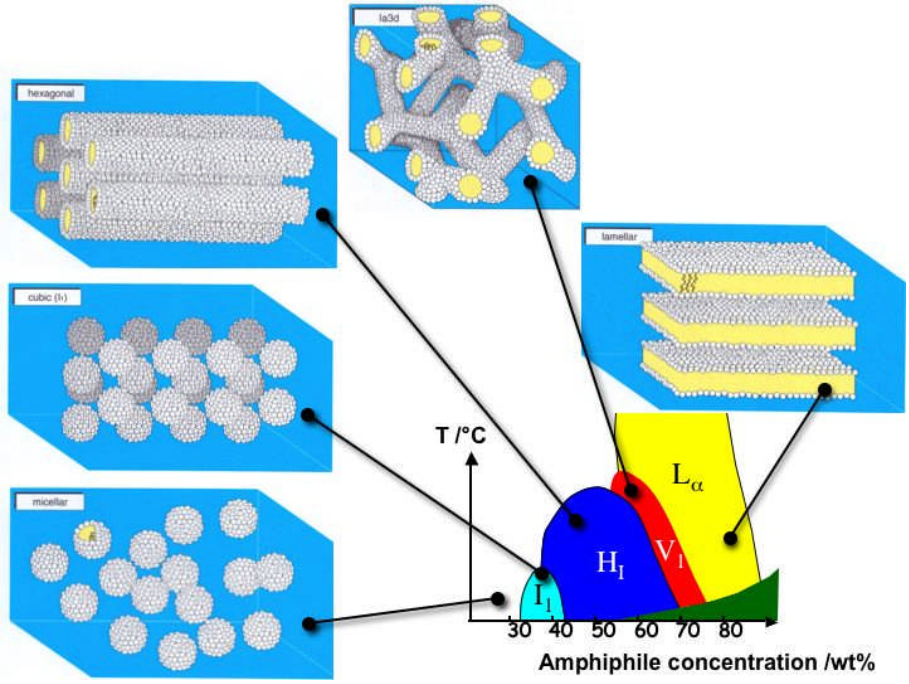

Figure 1.1, Schema of phase diagram in lyotropic system. Figure reproduced from reference [7].

1.2 Synthesis of mesoporous silica

The typical synthesis strategy of SMC is to use amphiphiles as structure-directing agents in aqueous solution due to their ability to self-assemble. Polymerization of a silica source will build up the walls around the amphiphilic aggregates. The driving force for formation relies on the interaction between the hydrophilic part of the amphiphile and the inorganic silica source.

The amphiphiles used in the synthesis are usually divided into two types: nonionic and ionic. The most frequently used nonionic amphiphiles are the triblock copolymer with the tradename Pluronic. They consist of two polyethylene oxide (PEO) blocks, that have a hydrophilic character, and one polypropylene oxide (PPO) block, with a more hydrophobic character. When the triblock copolymers are dissolved in aqueous solution above the critical micellar concentration (CMC) they form micelles via a self-assembly process. The hydrophobic part (the PPO block) will form the core of the micelle and the hydrophilic part (the PEO block) will mainly form the

corona surrounding the core. Pluronics are typically used for synthesis of the SBA family of mesoporous silicas,[8] for instance the well-known SBA-15 with 2D hexagonal structure.[9]

Ionic amphiphiles are characterized as cationic surfactants, with positively charged head groups, such as CTAB, and anionic surfactants, with negatively charged head groups, such as carboxylic and sulfonic head groups. Using cationic surfactants, SMCs with various structures have been synthesized. For instance, 2D hexagonal, micellar cubic, bi-continuous cubic and lamellar SMCs can be produced. MCM-41 with 2D hexagonal structure is an example of mesoporous silica material formed using a cationic surfactant.[5,6] As shown in Figure 1.2, it was described that the positively charged surfactant head group combines with the negatively charged silica species (under basic condistions) or positively charged silica species via intermediate anion such as Cl^- (under acidic conditions).[10] According to this scheme, the anionic head group should also be able to combine with the silica source at different ionization state. However, only lamellar or disordered mesophases resulted by using anionic surfactants. The probable reason was suggested to be that the anionic surfactant would mainly be protonated under acidic condition, while under basic condition the electrostatic interaction between the anionic surfactant and silicate ions would be too weak.[11]

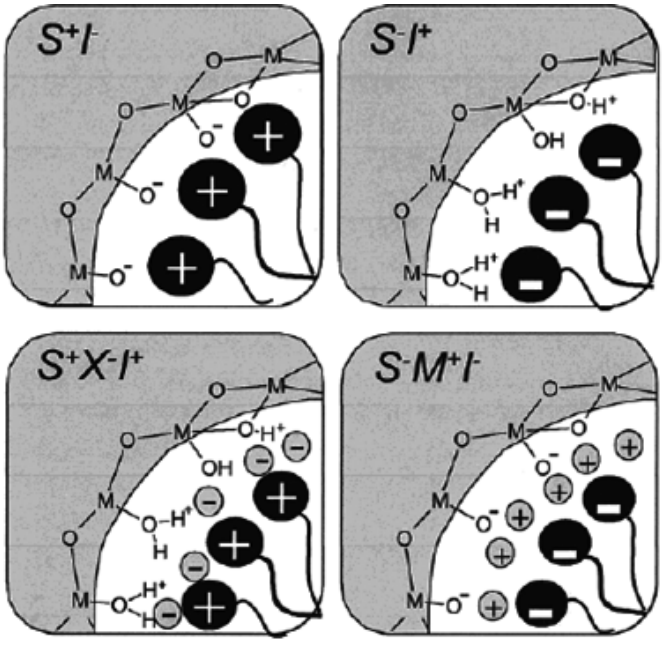

Figure 1.2, The suggested interactions between inorganic species and cationic or anionic surfactants in the formation of SMCs. Figure reproduced from reference [12].

In 2003, Che and co-workers reported a new method of synthesizing SMCs with anionic surfactants.[1] They introduced the concept of a co-structure directing agent (CSDA) into the

synthesis system, and many highly ordered SMCs, named anionic surfactant template mesoporous silicas (AMS), were produced by variation of the synthesis conditions.[13-16] The schematic synthesis strategy of AMS materials drawn by Che et al. is shown in Figure 1.3, which is explained to be based on electrostatic interactions between the organosilane and the surfactant headgroup. The organosilane is considered as a co-structure directing agent (CSDA). The silica source will polymerize around the organosilanes that have already paired with the surfactant head groups within the micelle. In the CSDA method, the mesostructure can be controlled by varying the ionization state of either the surfactant head group or the organic group part of the CSDA, i. e. a complicated but apparently very advantageous system, as many SMCs with different structures can be produced.

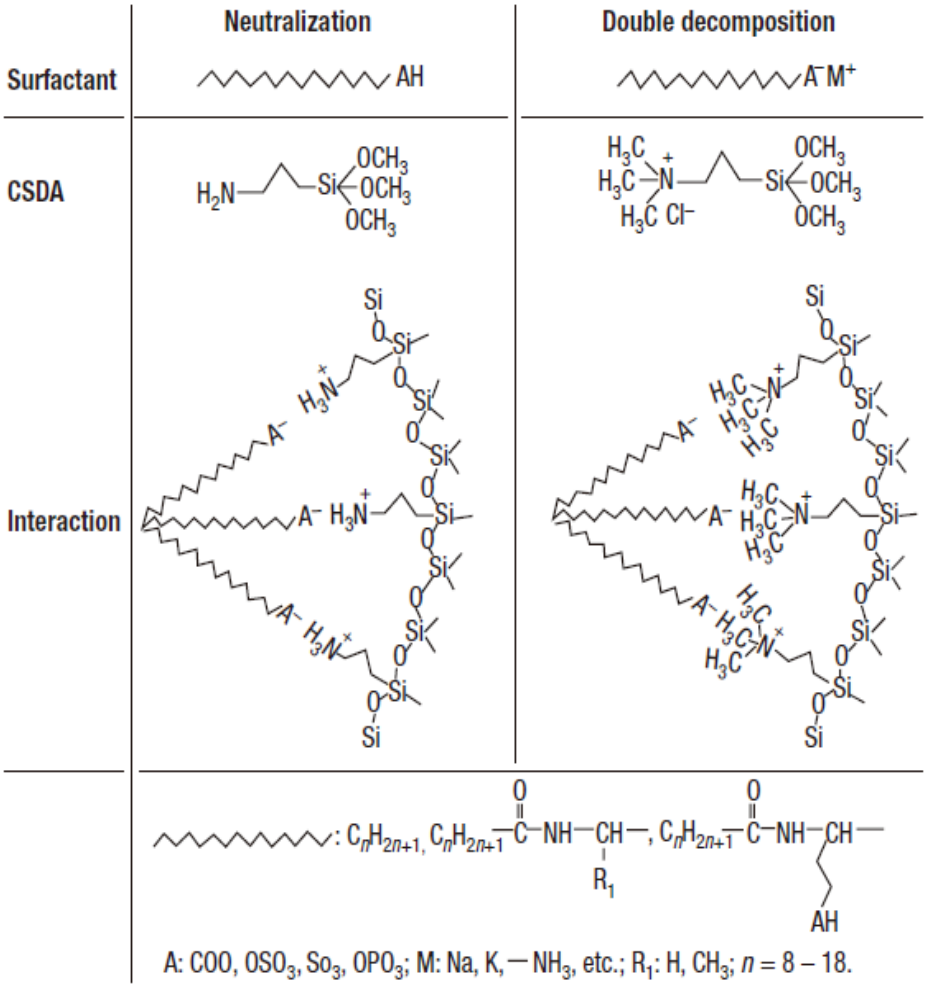

Figure 1.3, Schematic synthesis strategy of AMS materials by using CSDA. The illustration shows two CSDAs, 3-aminopropyltrimethoxysilane (APS) and *N*-trimethoxysilylpropyl-*N*,*N*,*N*-trimethylammonium chloride (TMAPS), and the corresponding between aminogroups and anionic surfactant head groups. Figure reproduced from reference [1].

1.3 Mesostructure types

As shown in Figure 1.1, amphiphiles organize in aqueous solutions to various liquid crystal types. The packing parameter of the surfactant is often used to describe which structure that is formed, for instance lamellar (bilayer), columnar (cylindrical) and micellar cubic (spherical). The packing parameter, $g = V/a_0 l$, where V is the total volume of the surfactant chains, a_0 is the effective head group area of the surfactant, and l the kinetic surfactant tail length, is used to describe the amphiphilc aggregations.[17,18] The bilayer structure has g value in the range $1/2 \leq g \leq 1$, cylindrical micelle has the value of $1/3 \leq g \leq 1/2$, and spherical micelle $g = 1/3$. Often this concept is also used for SMCs.

Various mesostructures have been discovered for SMCs. The mesostructures can be divided into different types. For example, with decreasing packing parameter, the mesotructure varies from lamellar to 2D columnar through bicontinuous cubic, and finally to cage-type cubic appear. Recently, a tri-continuous mesostructure has been reported.[19]

The lamellar mesostructured SMCs consist of layers of silica sheets with bilayer of amphiphiles in between. MCM-50 is a typical example of a lamellar structure. The 2D columnar mesostructure consists of rod-packing of long cylindrical micelles or packed molecules,[20] and includes the 2D hexagonal structure, with the plane group *p*6*mm*, the centered rectangular structure, with the plane group *c*2*mm*,[21] the 2D primitive rectangular structure, with the plane group *p*2*gg*,[22] and the 2D square structure with the plane group *p*4*mm*.[23] The 2D hexagonal structure (*p*6*mm*) is very common and is the structure defining MCM-41 and SBA-15. The bi-continuous cubic mesostructures have two disconnected but interwoven mesoporous networks divided by a silica wall. The silica wall lies on a minimal continuously curved surface. Three families of bi-continuous cubic mesostructures have been found to date. Their space groups are $Ia\bar{3}d$, $Pn\bar{3}m$ and $Im\bar{3}m$. MCM-48 is defined by $Ia\bar{3}d$. The cage-type mesostructures contain ordered or disordered packing of globular micelles. In the final silica materials the resulting pores sometimes have well-defined polyhedral shape.[24] Typically cage-type mesostructures are cubic, but other structures have also been reported. Space groups of $Fm\bar{3}m$, $P6_3/mmc$, $Im\bar{3}m$, $Pm\bar{3}n$, $Fd\bar{3}m$ and $P4_2/mnm$ are examples of this micellar structure type.

Usually, the packing parameter is suggested to describe the shape of the surfactant micelle. However, it does not describe the micellar packing. There are two simple concepts of regular lattices typically used to illustrate the dense packing of spherical micelles, cubic close-packed (CCP) and hexagonal close-packed (HCP) structures. They are well known as the structures having the highest packing density of ~0.74. Figure 1.4 shows the stacking of the two lattice forms. If the spheres (spherical micelles) in the bottom layer are in position A, the second layer

is in position B, the third layer can be either in position C or A. If the progression of stacking is ABC, the structure is CCP. If the stacking is ABA, the structure is HCP.

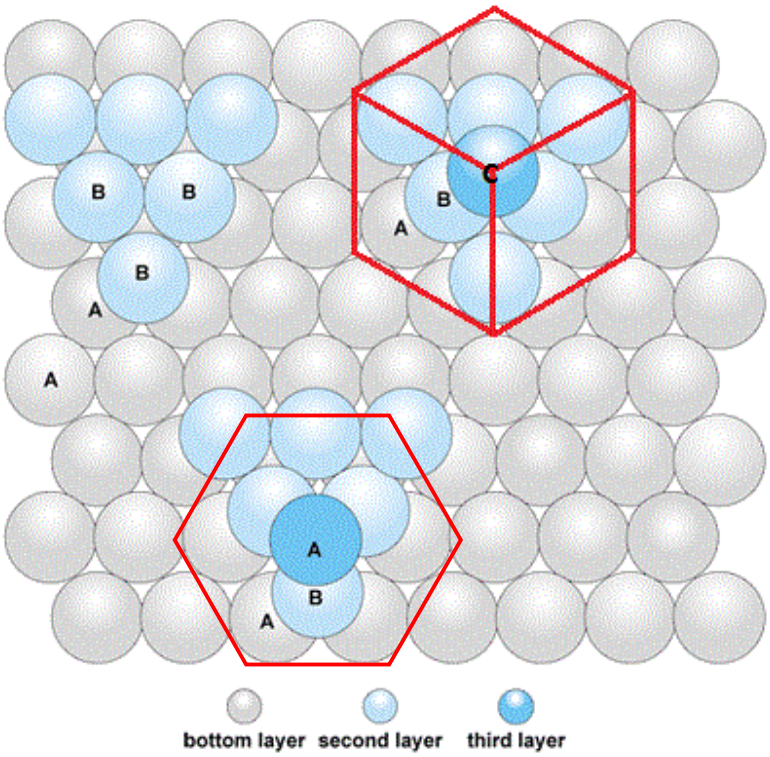

Figure 1.4, Schematic of the HCP lattice (down) and the CCP lattice (up right). Figure reproduced from reference [25].

In the case of SMCs with cage-type structure, the micelle is typically considered as spheres with packing parameter $g = 1/3$, and the interstices of the spheres are occupied by silica wall and the pores are connected by small windows on the contact area of the spherical micelles through the silica wall. $Fm\bar{3}m$ SMC has a CCP arrangement of a single type of spherical micelle regarded as perfect, or hard sphere (for instance SBA-12 [26]). However, the hard sphere model could not explain some of the cage-type structures, for example the structures with space group $Pm\bar{3}n$ and $Fd\bar{3}m$. The concept of polyhedron instead of perfect (hard) sphere has been introduced to explain this case. The spherical micelle is considered to make an interface with the next micelles and becomes a polyhedron instead of perfect (hard) sphere. This packing structure is called tetrahedrally close-packed (TCP) structure. For example, $Fd\bar{3}m$ structure can be described as a stacking of two kinds of layers made of two different polyhedra. As shown by Sakamoto and Han et al. in Figure 1.5, the unit cell (Fig.1.5, c) of $Fd\bar{3}m$ structure consists of sixteen dodecahedron (Fig.1.5, a) and eight 16-hedra (12 pentagons and 4 hexagons) (Fig.1.5, b). In the TCP-type SMCs, each polyhedron consists of both surfactant micelle and part of the silica wall (Fig.1.5, d).

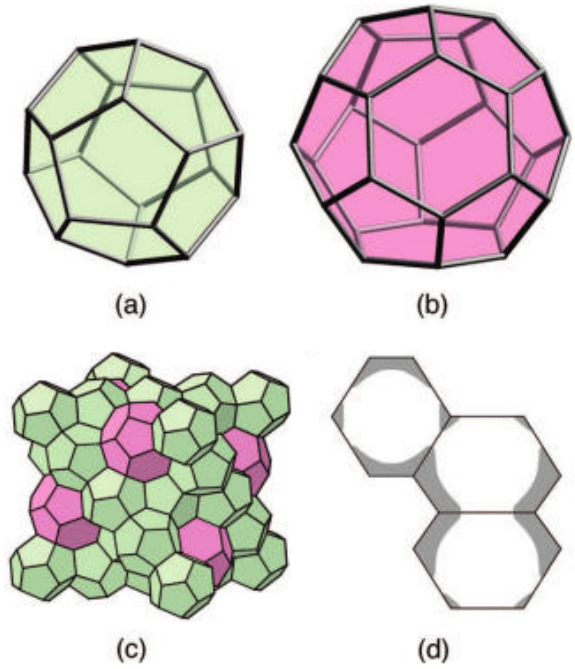

Figure 1.5, Schematic of (a): dodecahedron; (b): 16-hedron ($5^{12}6^4$-hedron); (c): the unit cell of Fd3m structure; (d): cages can be connected to each other through a window. Figure reproduced from reference [27].

1.4 Background

In 2007, Han et al. [2] found a new templating route for synthesizing carboxylic group functionalized mesoporous silicas (CFMSs). The strategy is based on the CSDA method (see 1.3), using cationic surfactant as template and carboxyethylsilanetriol sodium (CES; structure shown in Figure 1.6) as CSDA. Via this route, 3D structures of CFMSs were achieved by using the Gemini surfactant $C_{18\text{-}3\text{-}1}$ (Fig. 1.6), while by using the normal CTAB only 2D hexagonal structures were obtained. They explained this difference to arise as the headgroup area of the Gemini surfactant is bigger than CTAB, which leads to a smaller packing parameter.

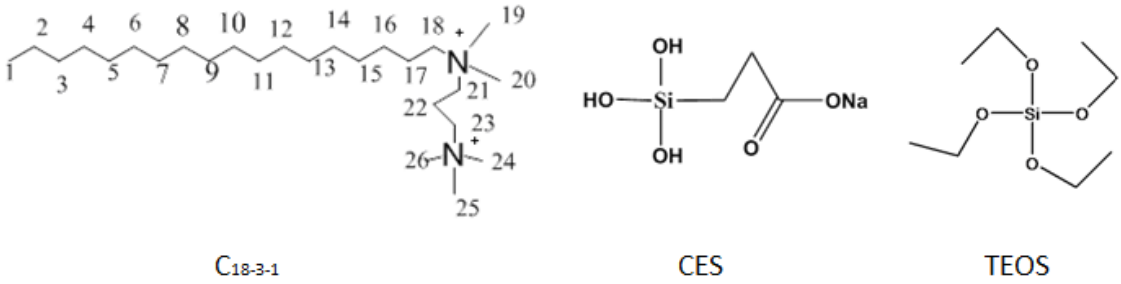

Figure 1.6, Molecular structures of $C_{18\text{-}3\text{-}1}$, CES and TEOS.

They tested the structural and morphological influence of concentration of the surfactant, amount of CES and addition of acid, [11] and reported a mesostructure transformation, from the $Fm\bar{3}m$ (Fig. 1.4) structure to $Fd\bar{3}m$ (Fig. 1.5) structure through a intergrowth structure, with increasing amount of HCl. Also interesting morphologies, such as hexagonal plate type, decahedral shape and so on, were obtained in these materials. Figure 1.7 shows the XRD patterns they reported of the CFMSs under different HCl concentrations. In addition, they mentioned that the sample with $Fm\bar{3}m$ structure is a mixture of CCP ($Fm\bar{3}m$) and HCP ($P6_3/mmc$) structure instead of pure $Fm\bar{3}m$ structure. CFMSs with pure $Fm\bar{3}m$ structures could only be synthesized with a very low surfactant concentration.

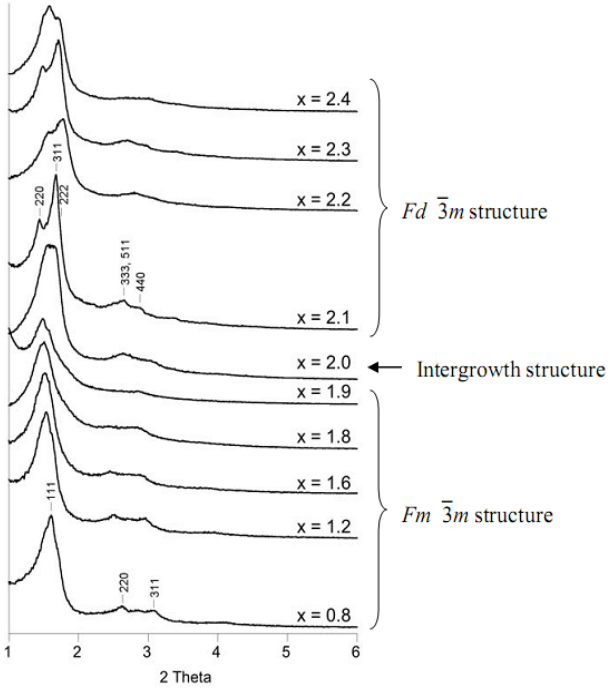

Figure 1.7, Powder XRD patterns of cage-type silica mesoporous crystals with the final composition, $C_{18\text{-}3\text{-}1}$: 2CES : xHCl : 15TEOS : 2000H_2O (x=0.8~2.4). Figure reproduced from reference [27 SI].

It was explained that the mesostructure changed because of the charge density of the wall surface changed with pH. In the case of high charge density of the wall, the hard sphere $Fm\bar{3}m$ structure was obtained, and with low charge density, the soft cages $Fd\bar{3}m$ structure was obtained. Figure 1.8 shows the proposed scheme, as suggested by Han et al.[2], of the interaction between the head groups of the surfactant, in this case with the gemini surfactant and the carboxylic groups of the CES. Because the carboxylic acids are weak acids, the ionization degree of the carboxylate site of CES can easily be controlled by different amounts of acid (e.g. HCl). When the acidity is low (pH 9.4~11.8, comparable with the pKa of silicic acid ($\equiv Si-OH$), ≈ 9.8) [28], CES is multivalent with both silicic acid part and carboxylate part, and interacts electrostatically with the cationic

ammonium groups of the surfactants and attached on the surface of the micelle. The large charge density on the micelle surface would also electrostatically drive the silica close to the micelle surface and result in the dense packing of silica, leading to hard sphere. On the other hand, the ionization of CSDA decreases when the acidity is increased to near neutral conditions by the addition of HCl (pH 5.7~5.8, larger than but comparable with the pKa of carboxylic acid, ≈ 5). The interaction between the carboxylate part of CES and the surfactant weakens, and the charge density on the micelle surface decreases, resulting in loose packing of soft cages.

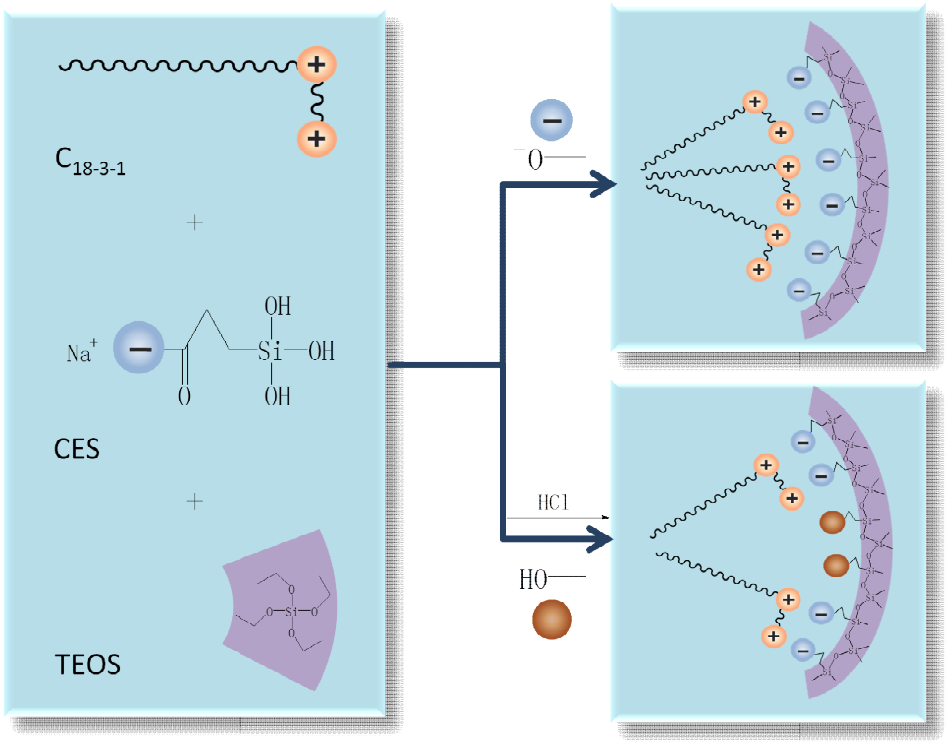

Figure 1.8, The proposed view on the interaction is given by Han et al.[2], illustrated with CTAB and CES. This figure illustrate the corresponding interaction with the gemini surfactant used in this master thesis work.

1.5 Aim of the work

In the work of Han et al.,[2,24,27] the structural transformation was explained to occur as a consequence of the pH changes. Here we explore if there is any other options to control the structural transformation and the material properties. As the formation mechanism has been explained to rely on the electrostatic interaction between the cationic surfactant and the anionic CSDA, we have explored how salt additions can influence the formation and the resulting material properties. The as-synthesized materials were investigated by SAXD and SEM. The pH of the synthesis solution was also recorded.

At first, we reproduced the CFMS materials reported by Han et al.[2], using $C_{18\text{-}3\text{-}1}$ as template, CES as CSDA. We obtained the structure transformation from $Fm\bar{3}m$ (mixed with $P6_3/mmc$) to $Fd\bar{3}m$, and also the expected morphologies of those materials.

Secondly, we added different amounts of NaCl (or $CaCl_2$) to syntheses performed at specific acid concentrations. The structures and the morphologies were investigated.

1.6 Characterization Techniques for SMCs

As mentioned in 1.1, the SMCs are considered as "cavity crystals", where the pores have long-range-ordering while the framework is amorphous. There are several main experimental techniques used to analyze the morphology, porosity and structure of the materials.

Typically, scanning electron microscope (SEM) is used to get the information about the surface topography, particle morphology and size of the SMCs. [29] Gas adsorption measurements are widely used for to determine the surface area and pore size distribution. [30] Small angle x-ray diffraction (SAXD) is the most common technique used to identify the structure of the SMCs. However, it is normally very difficult to determine the structure of the SMCs only by SAXD analysis. Transmission electron microscopy (TEM) is the most useful technique for structure determination. [31]

Small-angle X-ray Diffraction

Small angle X-ray Diffraction (SAXD) can be used to obtain the structural information about crystalline materials with a structural order in the size region from 1 to 100 nm. In general, because crystals are ordered 3-D periodic structures, the interaction of an x-ray beam with an array of planes of atoms will give rise to diffraction. The diffraction pattern is characteristic of the structure of the sample.

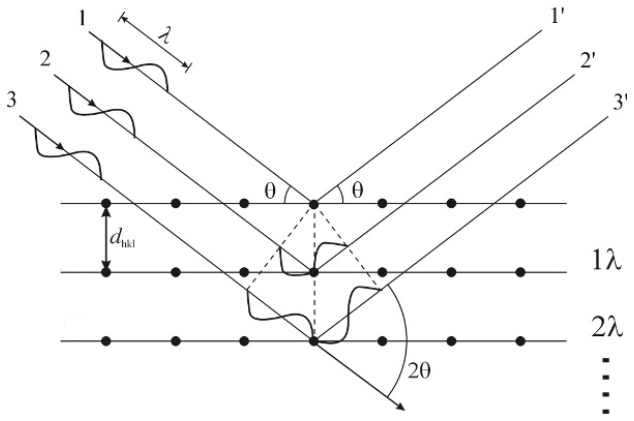

Figure 1.9, Schematic illustration of the reflection of X-rays from an ordered phase.

A simple geometrical picture can be used to explain the scattering of an X-ray beam by planes of atoms in an ordered phase, shown in Figure 1.9. Imagine the X-ray beam of wavelength λ, incident on the crystal at an angle θ. The interplanar distance is d. If the path length difference between X-rays scattered from different lattice-planes is an integer number of λ, constructive interference will be observed for X-rays that are reflected from the lattice planes at the reflected angle. This condition is summarized in Bragg's equation:

$$n\lambda = 2dsin\theta$$

where n is the integer (1, 2, 3...), λ is the wavelength of the X-ray beam, d is the interplanar distance and θ is the Bragg diffraction angle.

The SAXD analysed result is usually represented as a figure of the intensity as a function of the scattering vector q. The scattering vector q is related to d,

$$d = \frac{2\pi}{q}$$

The Miller indices ($h\ k\ l$) are used for the description of crystal planes and direction.[32] The triplet Miller indices, h, k and l, are three integer components but without any common denominator that uniquely characterise different planes as (hkl) in the structure. The Miller indices are related to the plane distance d. For instance, the relation between d and Miller indices for cubic crystal system is

$$\frac{1}{d^2} = \frac{h^2 + k^2 + l^2}{a^2}$$

and for hexagonal crystal system is

$$\frac{1}{d^2} = \frac{4}{3}\left(\frac{h^2 + hk + k^2}{a^2}\right) + \frac{l^2}{\mathrm{c}^2}$$

where a, c is the unit cell parameter that describe the lattice spacing.

When the SAXD instrument gives the pattern based on the scattering vector q, the Miller indices hkl can be identified by relation, for example,

$$q \propto \frac{1}{d} \propto \sqrt{h^2+k^2+l^2}$$

for cubic crystal system, and

$$q \propto \frac{1}{d} \propto \sqrt{h^2 + hk + k^2}$$

for 2D hexagonal crystal system.

The lattice spacing can also be calculated when hkl has been determined.

The space groups of the structures that are presented in this thesis is expected to be $Fm\bar{3}m$, $P6_3/mmc$ and $Fd\bar{3}m$. Based on the referenced XRD pattern of hexagonal $P6_3/mmc$, [33] cubic $Fm\bar{3}m$ [34] and $Fd\bar{3}m$[27 SI], the unique Miller Indices groups for these structures are shown in table 1. The structures of the samples can be identified by the ratios of the q values of different peaks from the pattern.

Table 1, Miller Indices groups of $P6_3/mmc$, $Fm\bar{3}m$ and $Fd\bar{3}m$, and the q ratios of different peaks.

Structures	Options	peak 1	peak 2	peak 3	peak 4	peak 5
$P6_3/mmc$ *	hkl	100	002	101	110	103
	q ratios	1	1.066	1.133	1.732	1.887
$Fm\bar{3}m$	hkl	111	200	220	311	222
	q ratios	1	1.155	1.633	1.915	2
$Fd\bar{3}m$	hkl	220	311	222	333, 511	440
	q ratios	1	1.173	1.225	1.837	2

*. For the hexagonal structure, the perfect HCP gives the lattice spacing $c/a = 1.633$, while c/a from the reference is 1.62, so here we set $c/a = 1.625$ to calculate the q ratios.

2. Experimental section

2.1 Synthesis

2.1.1 Chemicals

Tetraethyl orthosilicate (TEOS; from SCRC, Germany), and carboxyethylsilanetriol sodium salt (CES; from ABCR, Germany), were used as purchased without further purification. Gemini surfactant $[C_{18}H_{37}N(CH_3)_2(CH_3)_3N(CH_3)_3]Br_2$ ($C_{18\text{-}3\text{-}1}$) was obtained from and synthesized by Che's group, Shanghai Jiao Tong Univ., China. The molecular structures of these three chemicals are shown in Figure 1.6.

2.1.2 Synthesis of the material

The synthesis route used in this work uses $C_{18\text{-}3\text{-}1}$ as template, TEOS as silica source and CES as CSDA. A total of 1.40 g (2.5×10^{-4} mol) of $C_{18\text{-}3\text{-}1}$ was dissolved in MilliQ water followed by addition of 1M HCl and 1M NaCl (or $CaCl_2$) with different molar composition *x* (of HCl) and *y* (of NaCl or $CaCl_2$) separately, then 0.348 g (5×10^{-4} mol) of CES was added together with 0.78 g (3.75×10^{-3} mol) of TEOS. The final composition with molar ratios is $C_{18\text{-}3\text{-}1}$:2CES: xHCl: yNaCl($CaCl_2$): 15TEOS:2000H_2O, x=0~2.0, y=0~2.0. The mixture was stirred for 2 h at room temperature, and then hydrothermally reacted at 100^{o}C under static conditions for two days. The resultant white precipitates were collected by filtration and dried overnight at 80 ^{o}C (or at room temperature for two days).

2.2 Characterization

2.2.1 Small Angle X-ray Diffraction (SAXD)

SAXD patterns were detected by a 2D imaging plate detection system. The apparatus is implemented with a SAXSess camera using an X-ray generator (PANalytical, PW 3830) with a sealed copper tube. The X-ray generator offers a maximum power of 4.0 kW and an operating range of 20-60 kV and 10-100 mA. A Göbel mirror and a Kratky block collimation system (line-shaped beam) is used to convert the divergent polychromatic X-ray beam into a focused line shaped beam of Cu-Ka radiation (50 kV, 40 mA).

2.2.2 Scanning Electron Microscopy (SEM)

The microscopic features of the sample were observed with a JEOL JSM-6700 instrument with a thin layer of gold coating, operating at 10 kv.

3. Results and discussions

3.1 Synthesis of CFMSs Synthesized with $C_{18\text{-}3\text{-}1}$

As mentioned in the introduction section, Han at el. reported that CFMSs synthesized with $C_{18\text{-}3\text{-}1}$ via CSDA method showed a mesostructure transformation from the $Fm\bar{3}m$ (mixed with $P6_3/mmc$) structure to the $Fd\bar{3}m$ structure by increasing the amount of HCl in the synthesis.[2] These materials were reproduced in this thesis. Different amounts of HCl were added in to the synthesis system. The molar ratios were $C_{18\text{-}3\text{-}1}$: 2CES: xHCl: 15TEOS: $2000H_2O$, x=0~2.0. Here, we discuss the samples with HCl molar ratios of 0.8, 1.0, 1.2, 1.4, 1.6, 1.7 and 1.8.

3.1.1 Structure analysis

The structures of the samples are supposed to be $Fm\bar{3}m$ or $Fd\bar{3}m$. The $Fm\bar{3}m$ structure typically occurs with more or less intergrowth of the $P6_3/mmc$ structure, as explained in Section 1.4. It is easy to analyse the structures by using SAXD. The SAXD patterns of the as-made mesoporous silicas synthesized using different HCl/$C_{18\text{-}3\text{-}1}$ molar ratios are shown in Figure 3.1.1.

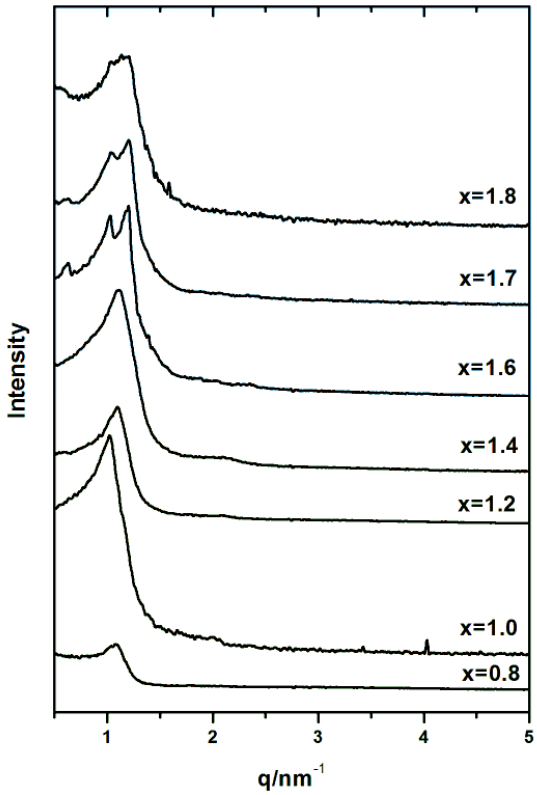

Figure 3.1.1, SAXD pattern of the as-made CFMSs by using $C_{18\text{-}3\text{-}1}$ as template. The reaction molar composition was $C_{18\text{-}3\text{-}1}$:CES:HCl:TEOS:H2O=1:2:x:15:2000, where x= 0.8~1.8.

When HCl/$C_{18\text{-}3\text{-}1}$ molar ratio is below 1.2, the SAXDs show similar patterns, which can be inferred that samples with HCl/$C_{18\text{-}3\text{-}1}$=0.8, 1.0 and 1.2 contain the same structures. Similarly, when HCl/$C_{18\text{-}3\text{-}1}$ molar ratio is above 1.6, the SAXDs assume same structures. Figure 3.1.2 shows the peak indexed with Miller Indices of different structures for the samples with HCl/$C_{18\text{-}3\text{-}1}$ molar ratios of 1.2, 1.4 and 1.6.

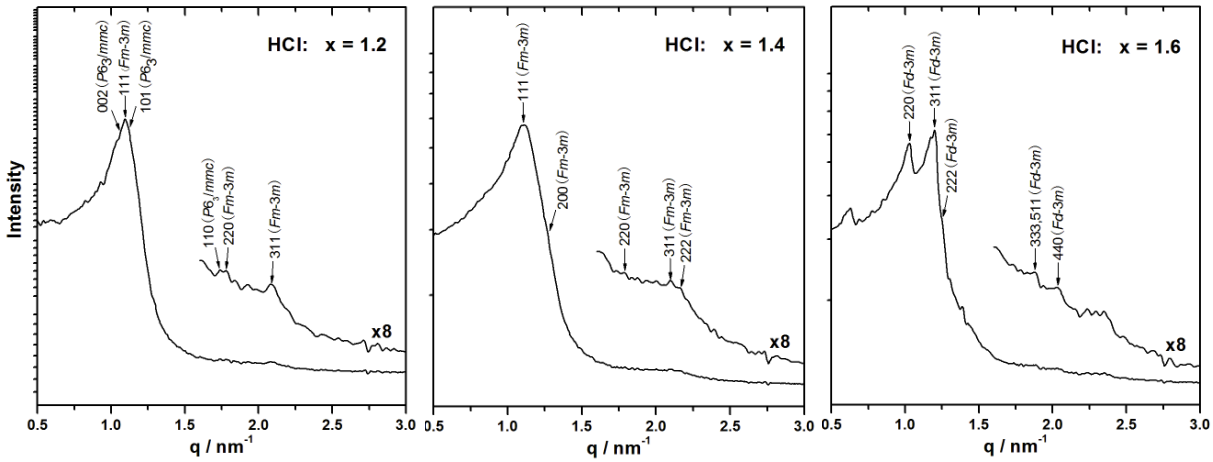

Figure 3.1.2, The peak indexed with Miller Indices of different structures for the samples with HCl/$C_{18\text{-}3\text{-}1}$ molar ratios of 1.2, 1.4 and 1.6.

After calculating the ratios of q values from different peaks of the SAXD pattern, the structures of different samples have been identified. For the SAXD pattern of sample with HCl/$C_{18\text{-}3\text{-}1}$ molar ratio of 1.2, the peaks from the $Fm\bar{3}m$ structure and $P6_3/mmc$ structure are indexed. The structure of the sample is likely a combination of both $Fm\bar{3}m$ and $P6_3/mmc$ structures. When HCl/$C_{18\text{-}3\text{-}1}$=1.4, the SAXD pattern shows the peaks of the $Fm\bar{3}m$ structure. But, the 111 peak is very wide and all the following peaks are not very clear. The probable reason is that it is an intergrowth structure. When HCl/$C_{18\text{-}3\text{-}1}$=1.6, there are clear peaks of the $Fd\bar{3}m$ structure shown in the SAXD pattern.

Therefore, from the reproduced results, with increasing the amount of HCl in the synthesis system, the structure transform from $Fm\bar{3}m$ (mixed with $P6_3/mmc$) (x=0.8, 1.0, 1.2) to $Fd\bar{3}m$ (x=1.6, 1.7, 1.8) structure possibly through a intergrowth structure (x=1.4). These results show the same transformation from the work of Han et al.

The pH measurements have also been done for the reproduced samples before the reaction (addition of CES and TEOS) and after the reaction (2 hours after adding CES and TEOS), the results are shown in Appendix 1.1. The final pH values for $Fm\bar{3}m$ (mixed with $P6_3/mmc$) structures are above 8.6, for the $Fd\bar{3}m$ structures are below 6, and for the intergrowth structure of $Fm\bar{3}m$ and $Fd\bar{3}m$, it is in between.

3.1.2 Morphologies

Morphologies of CFMSs synthesized by using $C_{18\text{-}3\text{-}1}$ as template were checked by SEM. Both overview and higher magnification images of the as-made samples at the molar ratio of $C_{18\text{-}3\text{-}1}$: 2CES: xHCl: 15TEOS: 2000H_2O, x=0.8~1.8, are shown in Appendix 1.3. Figure 3.1.3 shows the SEM images with high magnification of those samples.

The samples with HCl/$C_{18\text{-}3\text{-}1}$ molar ratios of 0.8, 1.0 and 1.2, which are supposed to have the combined $Fm\bar{3}m$ and $P6_3/mmc$ structures, and the samples with HCl/$C_{18\text{-}3\text{-}1}$=1.4, which could be the intergrowth structure, show roundish morphologies. However, the roundish shaped particles do not show crystalline faces. It is likely because that the samples do not contain pure structures and it is therefore difficult to form well defined morphologies. The roundish particles from different samples become bigger when the HCl concentration increases in the synthesis system.

The samples with HCl/$C_{18\text{-}3\text{-}1}$ molar ratios of 1.6, 1.7 and 1.8 (the $Fd\bar{3}m$ structures), show well defined but not uniform crystalline morphologies. When HCl/$C_{18\text{-}3\text{-}1}$=1.6, the morphology is a mix of hexagonal and layered particles. For HCl/$C_{18\text{-}3\text{-}1}$=1.7, not only hexagonal but also cubic particles appear. While when HCl/$C_{18\text{-}3\text{-}1}$=1.8, the particles show more triangle faces. Since the $Fd\bar{3}m$ structure is a face centered cubic structure, all those morphologies are reasonable. Moreover, there are a lot of small “fluffy” particles shown in the SEM image when the HCl molar ratio of 1.8 to $C_{18\text{-}3\text{-}1}$. Possibly the pH is too high at this HCl concentration that the silica source could not aggregate during the reaction.

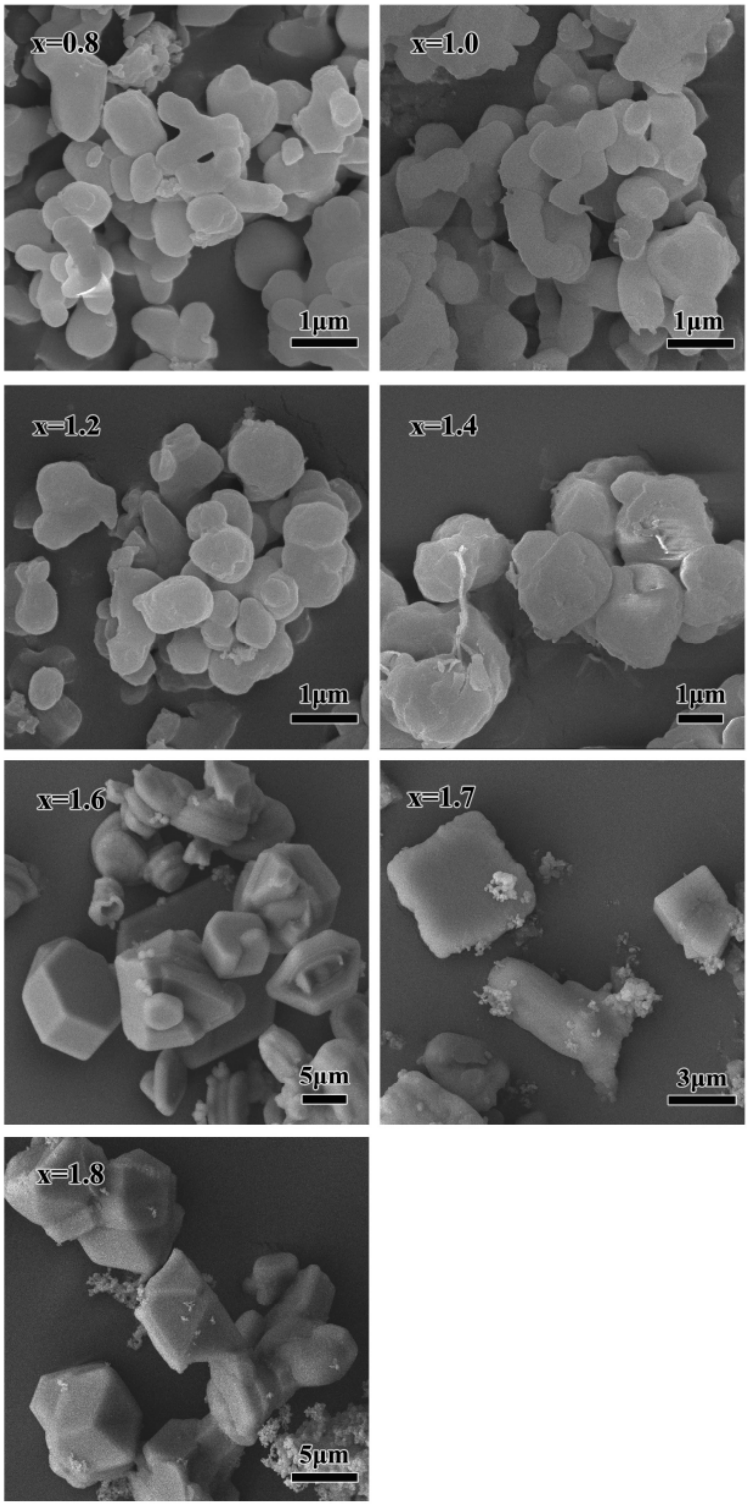

Figure 3.1.3, SEM images of the as-made CFMSs by using $C_{18\text{-}3\text{-}1}$ as template. The reaction molar composition was $C_{18\text{-}3\text{-}1}$: CES: HCl: TEOS: H_2O=1:2:x:15:2000, where x= 0.8~1.8.

3.2 Influence of sodium chloride

Besides the pH influence, salt influence was investigated for synthesis of CFMSs using $C_{18\text{-}3\text{-}1}$ as template in our work. Different amounts of NaCl were added in to the synthesis system at HCl molar ratios of 1.0, 1.2, 1.4, 1.6 and 1.7 to $C_{18\text{-}3\text{-}1}$. The molar ratios were $C_{18\text{-}3\text{-}1}$: 2CES: xHCl: yNaCl: 15TEOS: 2000H_2O, x=1.0~1.7, y=0.0~2.0. All the pH, SAXD and SEM measurement results are shown in Appendix 2. Here, we discuss the samples with HCl/$C_{18\text{-}3\text{-}1}$=1.2, 1.4 and 1.6.

3.2.1 Hydrochloric acid molar ratio of 1.2 to $C_{18\text{-}3\text{-}1}$

From the reproduction work, when HCl/$C_{18\text{-}3\text{-}1}$=1.2, the structure of the sample is supposed to be a mixture of the $Fm\bar{3}m$ and $P6_3/mmc$ structure. The SAXD patterns of the as-made mesoporous silicas synthesized using different NaCl/$C_{18\text{-}3\text{-}1}$ molar ratios are shown in Figure 3.2.1.

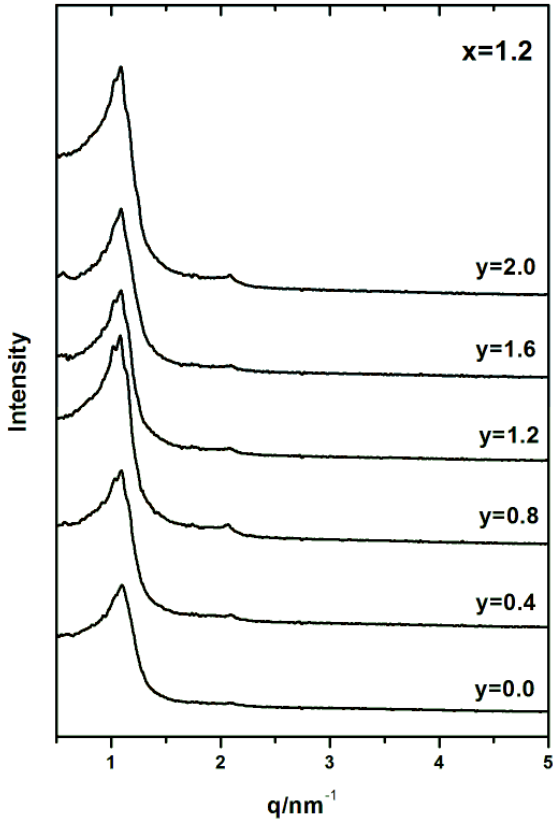

Figure 3.2.1, SAXD pattern of the as-made CFMSs by using $C_{18\text{-}3\text{-}1}$ as template and with addition of NaCl. The reaction molar composition was $C_{18\text{-}3\text{-}1}$: CES: HCl: NaCl: TEOS: H2O = 1: 2: x: y: 15: 2000, where x= 1.2, y= 0.0~2.0.

All the samples with different NaCl concentrations show quite similar SAXD patterns. However, by calculating the *q* value from different peaks, there are slight differences between the SAXD

patterns. Figure 3.2.2 shows the peak indexed with Miller Indices of different structures for the samples with NaCl/$C_{18\text{-}3\text{-}1}$ molar ratios of 0.0 and 2.0.

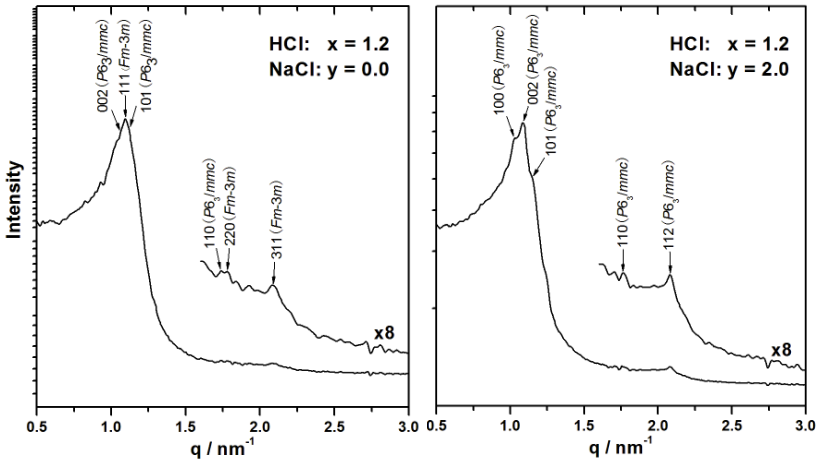

Figure 3.2.2, The peak indexed with Miller Indices of different structures for the samples with HCl/$C_{18\text{-}3\text{-}1}$ molar ratio of 1.2, and NaCl/$C_{18\text{-}3\text{-}1}$ molar ratios of 0.0 and 2.0.

When NaCl/$C_{18\text{-}3\text{-}1}$=2.0, the expected peaks from the *P*6$_3$/*mmc* structure are observed in the SAXD pattern. However, the *q* ratios of the 111, 220 and 311 peaks from the $Fm\bar{3}m$ structure are similar to the *q* ratios of the 002, 110 and 112 peaks from the *P*6$_3$/*mmc* structure. So, it is difficult to say if the structure of this sample is pure *P*6$_3$/*mmc* structure or if it is combined with the $Fm\bar{3}m$ structure.

Figure 3.2.3 shows the SEM images of the as-made CFMS samples synthesized at the molar ratio of $C_{18\text{-}3\text{-}1}$:CES:HCl:NaCl:TEOS:H_2O=1:2:x:y:15:2000, x=1.2, y=0.0, 0.8 and 2.0.

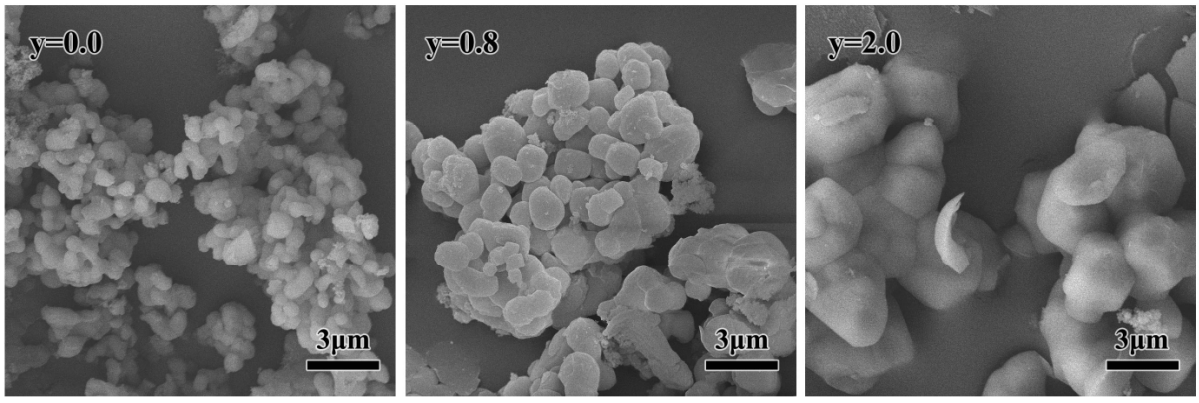

Figure 3.2.3, SEM images of the as-made CFMSs by using $C_{18\text{-}3\text{-}1}$ as template and with addition of NaCl. The reaction molar composition was $C_{18\text{-}3\text{-}1}$: CES: HCl: NaCl: TEOS: H_2O = 1: 2: x: y: 15: 2000, where x=1.2, y=0.0, 0.8 and 2.0.

Roundish morphologies are observed in the SEM images. While in comparison to the samples with lower NaCl concentration, in the sample with NaCl molar ratio of 2.0 to $C_{18\text{-}3\text{-}1}$, the morphology shows more crystalline faces. It is probably because the sample with NaCl/$C_{18\text{-}3\text{-}1}$ molar ratio of 2.0 is structurally more pure than the other samples. The morphology results correspond to the SAXD information. Additionally, with increasing the amount of NaCl, the particle size increases.

3.2.2 Hydrochloric acid molar ratio of 1.4 to $C_{18\text{-}3\text{-}1}$

When the HCl molar ratio to $C_{18\text{-}3\text{-}1}$ is 1.4, a progress of structure transformation has been obtained. The SAXD patterns of the as-made mesoporous silicas synthesized using different NaCl/$C_{18\text{-}3\text{-}1}$ molar ratios are shown in Figure 3.2.4.

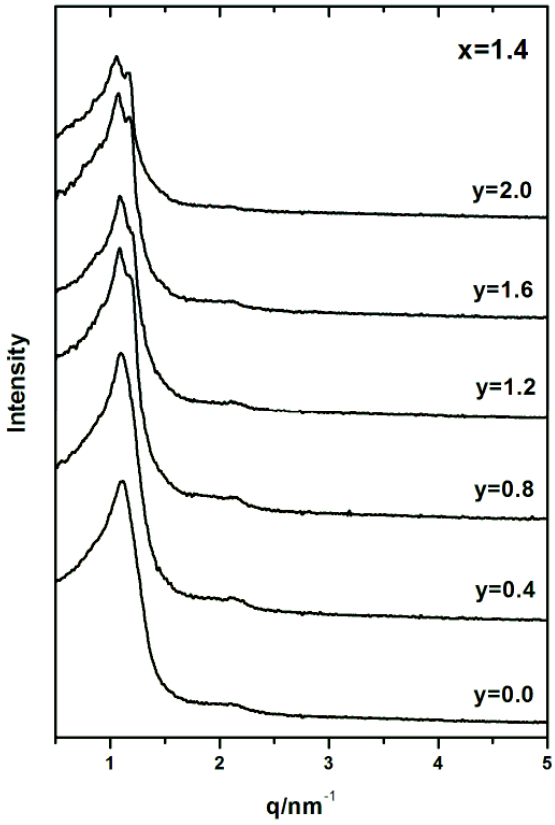

Figure 3.2.4, SAXD pattern of the as-made CFMSs by using $C_{18\text{-}3\text{-}1}$ as template and with addition of NaCl. The reaction molar composition was $C_{18\text{-}3\text{-}1}$: CES: HCl: NaCl: TEOS: H2O = 1: 2: x: y: 15: 2000, where x= 1.4, y= 0.0~2.0.

Figure 3.2.5 shows the peak indexed with Miller Indices of different structures for the samples with NaCl/$C_{18\text{-}3\text{-}1}$ molar ratios of 0.0 and 2.0. As discussed in the reproduction part, the reproduced CFMS sample with NaCl/$C_{18\text{-}3\text{-}1}$=1.4 is supposed to have the $Fm\bar{3}m$ structure

(probably with an intergrowth of the $Fd\bar{3}m$ structure). When NaCl/$C_{18\text{-}3\text{-}1}$=2.0, peaks of both $Fm\bar{3}m$ and $Fd\bar{3}m$ structures are found from the SAXD pattern. There are also several unclear peaks possibly belonging to the $P6_3/mmc$ structure. With an increasing of the NaCl concentration, the samples contain more and more $Fd\bar{3}m$ structure. Moreover, the 222 peak of the $Fm\bar{3}m$ structure is very clear. Considering that the q value of the 222 peak from the $Fm\bar{3}m$ structure is twice that of the highest 111 peak, there is also a possibility that this sample contains a lamellar structure. Indicating a complicated structure composition is shown in this group of samples.

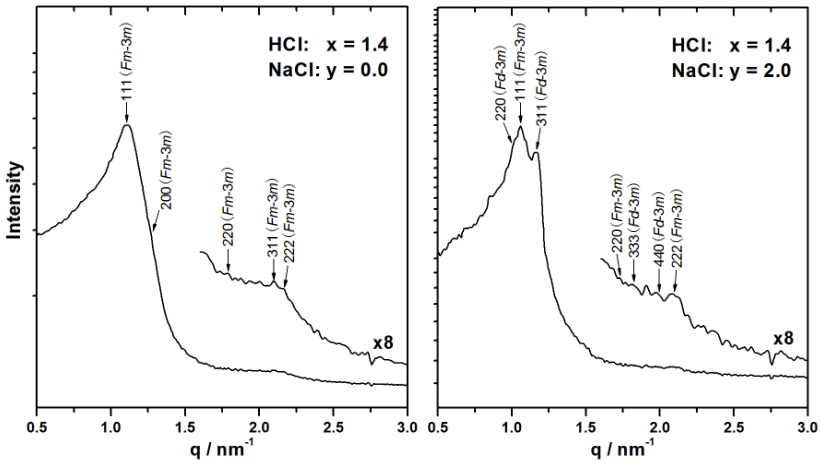

Figure 3.2.5, The peak indexed with Miller Indices of different structures for the samples with HCl/$C_{18\text{-}3\text{-}1}$ molar ratio of 1.4, and NaCl/$C_{18\text{-}3\text{-}1}$ molar ratios of 0.0 and 2.0.

Figure 3.2.6 shows the SEM images with magnifications of the as-made CFMS samples that synthesized at the molar ratio of $C_{18\text{-}3\text{-}1}$:CES:HCl:NaCl:TEOS:H_2O=1:2:x:y:15:2000, x=1.4, y=0.0~2.0. The overview SEM images of this group of samples are shown in Appendix 2.3.

As the NaCl concentration increase, the morphologies of the samples show more and more crystalline faces. At low concentration of NaCl, the particles are roundish with unclear faces. Very thin layers could also be found in the non-uniform materials. Those layers are supposed to have the lamellar structure that could possibly explain the high intensity 222 peak of the $Fm\bar{3}m$ structure from the SAXD pattern. When NaCl/$C_{18\text{-}3\text{-}1}$=1.6, the morphology is layered and can be indicative of stacking faults. When NaCl molar ratio to $C_{18\text{-}3\text{-}1}$ is 2.0, well defined plate shaped hexagonal morphologies are obtained, an indication for the structure of this sample being purer. The structure transformation from the $Fm\bar{3}m$ structure to an intergrowth structure is also consistent with the SEM images.

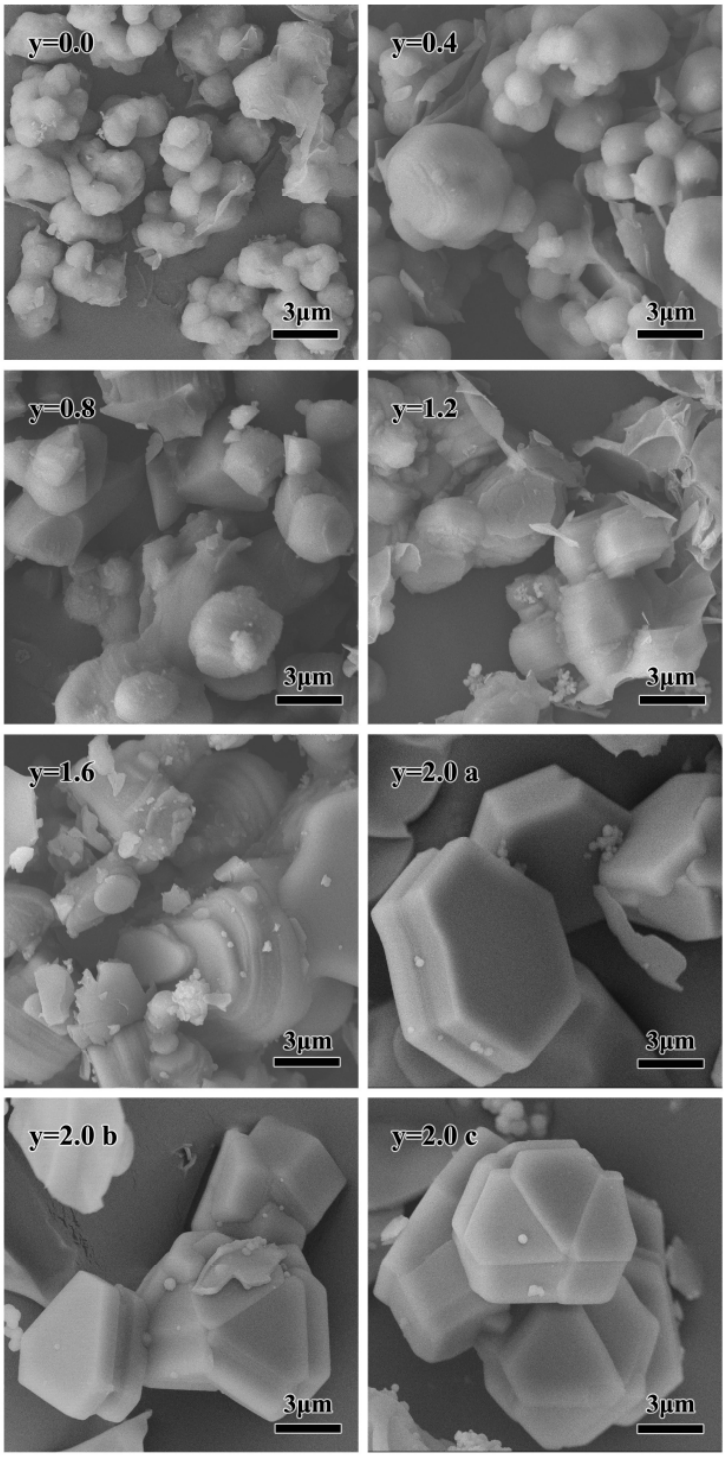

Figure 3.2.6, SEM images of the as-made CFMSs by using $C_{18\text{-}3\text{-}1}$ as template and with addition of NaCl. The reaction molar composition was $C_{18\text{-}3\text{-}1}$: CES: HCl: NaCl: TEOS: H_2O = 1: 2: x: y: 15: 2000, where x=1.4, y=0.0~2.0.

3.2.3 Hydrochloric acid molar ratio of 1.6 to $C_{18\text{-}3\text{-}1}$

Clear $Fd\bar{3}m$ structures are defined for the group of samples when the HCl molar ratio to $C_{18\text{-}3\text{-}1}$ is 1.4. As shown in the composition table (Appendix 2.4), only the lattice spacing is slightly different from each sample. The SAXD patterns of the as-made mesoporous silicas synthesized using different NaCl/$C_{18\text{-}3\text{-}1}$ molar ratios are quite similar (as shown in Figure 3.2.7).

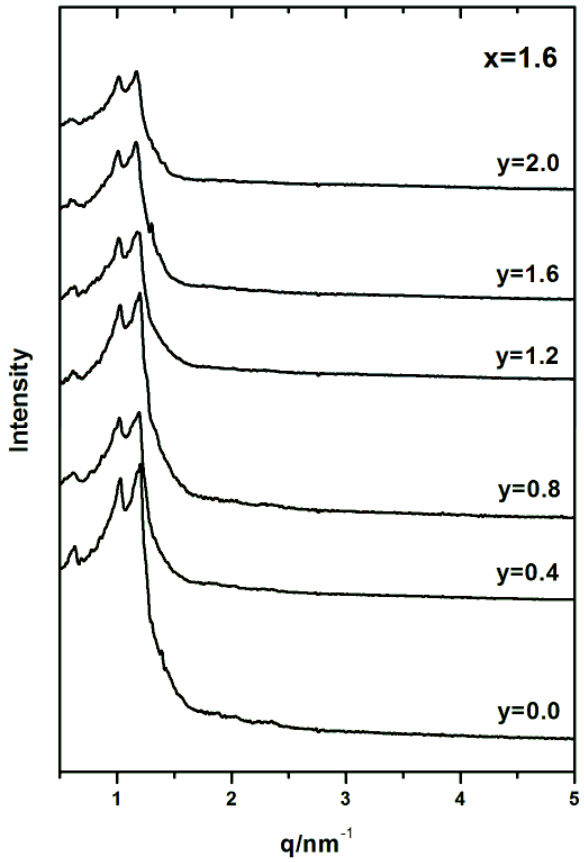

Figure 3.2.7, XRD pattern of the as-made CFMSs by using $C_{18\text{-}3\text{-}1}$ as template and with addition of NaCl. The reaction molar composition was $C_{18\text{-}3\text{-}1}$: CES: HCl: NaCl: TEOS: H2O = 1:2: x: y: 15: 2000, where x= 1.6, y= 0.0~2.0.

Figure 3.2.8 shows the SEM images with magnifications of the as-made CFMS samples that synthesized at the NaCl/$C_{18\text{-}3\text{-}1}$ molar ratio of 0.0, 0.8 and 2.0. The overview SEM images of this group of samples are shown in Appendix 2.4.

Well defined hexagonal plate shaped particles are found in the morphologies. Well defined cubic particles are also obtained as NaCl concentration increasing.

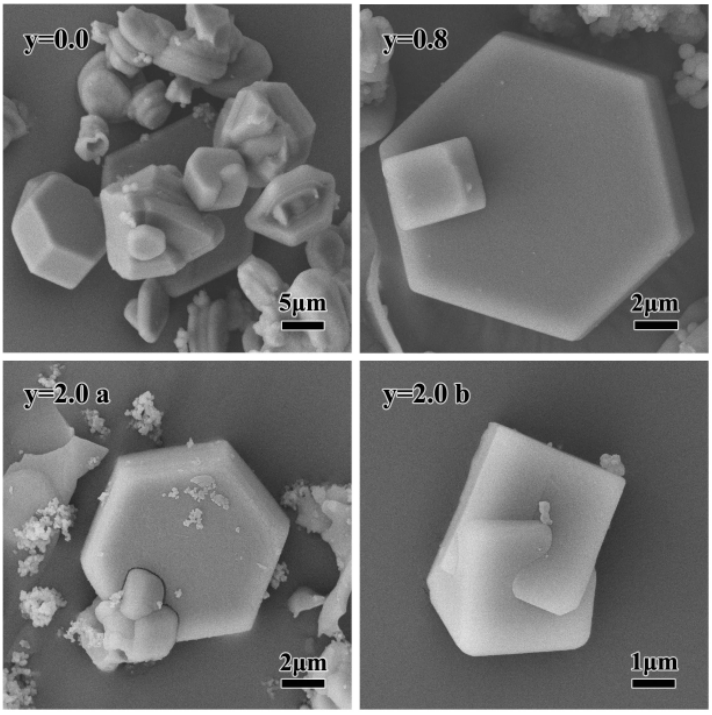

Figure 3.2.8, SEM images of the as-made CFMSs by using $C_{18\text{-}3\text{-}1}$ as template and with addition of NaCl. The reaction molar composition was $C_{18\text{-}3\text{-}1}$: CES: HCl: NaCl: TEOS: H_2O = 1: 2: x: y: 15: 2000, where x=1.6, y=0.0, 0.8 and 2.0.

3.2.4 Summary

The influences when adding NaCl into the synthesis system of CFMSs could be separated as a structural influence and a morphology influence.

In order to explain the structure influence, a synthesis diagram has been drawn based on the different molar ratios of HCl vs. NaCl, shown in Figure 3.2.9. When the HCl/$C_{18\text{-}3\text{-}1}$ molar ratios are below 1.2, all the samples are consistent with the $Fm\bar{3}m$ structure (mixed with the $P6_3/mmc$ structure). When HCl/$C_{18\text{-}3\text{-}1}$=1.2, with increasing of the concentration of NaCl, the structure has been indexed as $P6_3/mmc$ since no peak was found from the $Fm\bar{3}m$ structure. But it is likely an intergrowth which is dominated by the $P6_3/mmc$ structure. A structure transformation occurs when HCl/$C_{18\text{-}3\text{-}1}$=1.4, from the $Fm\bar{3}m$ structure to the intergrowth with the $Fd\bar{3}m$ structure, with increasing of the amounts of NaCl. While when the HCl molar ratios to $C_{18\text{-}3\text{-}1}$ increase above 1.6, the structures of the samples remain as the $Fd\bar{3}m$ structure. So the structure transformation has only been influenced by NaCl in a small region of the amounts of HCl, around the HCl/$C_{18\text{-}3\text{-}1}$ molar ratio of 1.4.

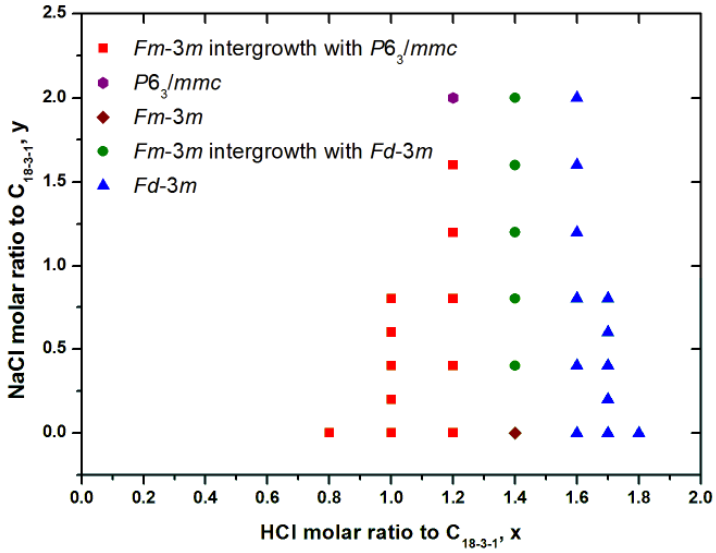

Figure 3.2.9, Synthesis diagram of the CFMSs synthesis system with NaCl influence.

Since the addition of NaCl mainly increase the ionic strength without changing pH in the synthesis system. The ionic strengths and the pH measurements of different samples are shown in the Appendix. Figure 3.2.10 shows a structure diagram about the relation between ionic strength and pH in the synthesis system. When the pH values are above 8.5, almost all the samples have the $Fm\bar{3}m$ structures (mixed with the $P6_3/mmc$ structures). A dominated $P6_3/mmc$ structure has been obtained at a very large ionic strength in this pH region. When the pH values are below 6, all the samples have the $Fd\bar{3}m$ structures. During the pH region between 6 and 8.5, the structures of the samples transform from the $Fm\bar{3}m$ structures to the intergrowth structures as the ionic strength increasing.

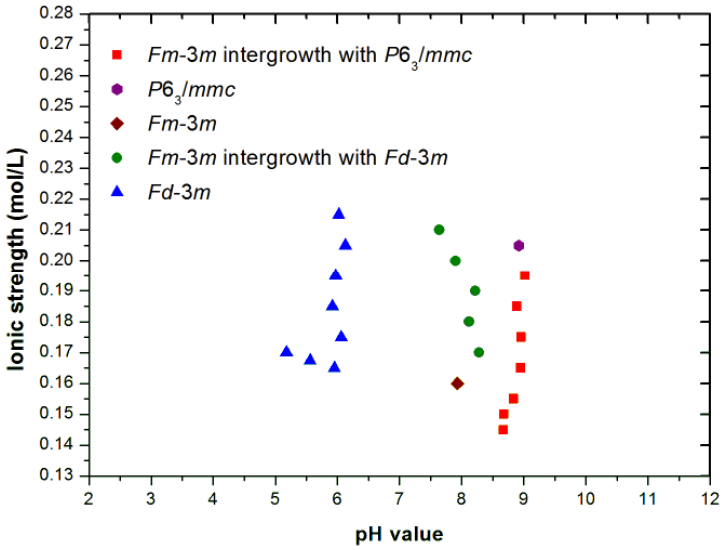

Figure 3.2.10, pH vs. ionic strength

Summarizing the SEM results of CFMS samples with addition of NaCl, the morphology of the materials usually follows the structure. When the samples are supposed to have pure structures, the SEM images show morphologies with crystalline faces. It is also observed that the particle size increases with the amounts of NaCl.

The SEM images of the sample with the molar ratio $HCl/C_{18\text{-}3\text{-}1}$=1.7 and $NaCl/C_{18\text{-}3\text{-}1}$=2.0 and the sample of the molar ratio $HCl/C_{18\text{-}3\text{-}1}$=1.8 are shown in Figure 3.2.11. The morphologies of both these samples show similar particles with triangle faces. The sample with higher concentration of acid contains a lot of small "fluffy" particles, as mentioned previously. For the sample at lower acid concentration but with NaCl, no unexpected "fluffy" particle was found. Hence, well defined morphologies can be achieved by increasing the salt concentration in the synthesis system.

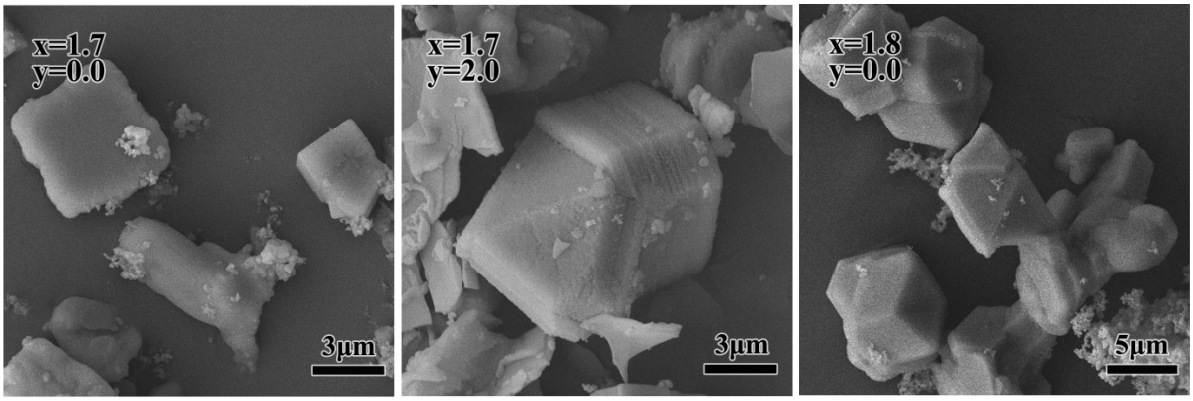

Figure 3.2.11, SEM images of the as-made CFMSs by using $C_{18\text{-}3\text{-}1}$ as template and with addition of NaCl. The reaction molar composition was $C_{18\text{-}3\text{-}1}$: CES: HCl: NaCl: TEOS: H_2O = 1: 2: x: y: 15: 2000, where x=1.7 and 1.8, y=0.0 and 2.0.

3.3 Influence of calcium chloride

Since the ionic strength could be a reason for the structure transformation, a divalent calcium salt has been added to the CFMSs synthesis system. In order to be comparable with the experiments of the addition of NaCl, same amounts of $CaCl_2$ with $CaCl_2/C_{18\text{-}3\text{-}1}$ molar ratios of 0.0~2.0 are added at typical $HCl/C_{18\text{-}3\text{-}1}$ molar ratios of 1.2, 1.4 and 1.6. However, the amounts of CES are added differently for the samples when $HCl/C_{18\text{-}3\text{-}1}$=1.4 and1.6, so these samples will only be compared within the group themselves.*

3.3.1 Hydrochloric acid molar ratio of 1.2 to $C_{18\text{-}3\text{-}1}$

When the HCl molar ratio to $C_{18\text{-}3\text{-}1}$ is 1.2, the results are comparable to the samples with addition of NaCl. The SAXD patterns of the as-made mesoporous silicas synthesized using different $CaCl_2/C_{18\text{-}3\text{-}1}$ molar ratios (Figure 3.2.7) are very similar to the SAXD patterns at the same $HCl/C_{18\text{-}3\text{-}1}$ molar ratio with different NaCl concentration. The structures of this group of samples are the $Fm\bar{3}m$ structures possibly with intergrowths of the $P6_3/mmc$ structures.

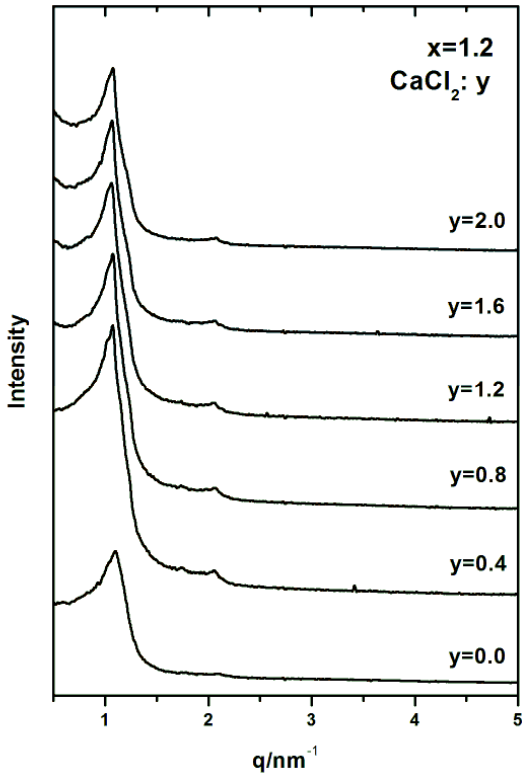

Figure 3.3.1, XRD pattern of the as-made CFMSs by using $C_{18\text{-}3\text{-}1}$ as template and with addition of $CaCl_2$. The reaction molar composition was $C_{18\text{-}3\text{-}1}$: CES: HCl: $CaCl_2$: TEOS: H2O = 1:2: x: y: 15: 2000, where x= 1.2, y= 0.0~2.0

* The CES used in these samples are from another batch, which had a different density (of the CES).

The SEM images with high magnifications of the sample at $HCl/C_{18\text{-}3\text{-}1}$ molar ratio of 1.2 without addition of salt and the samples with addition of NaCl and $CaCl_2$ when $NaCl/C_{18\text{-}3\text{-}1}$ (or $CaCl_2/C_{18\text{-}3\text{-}1}$) = 2.0 are shown in Figure 3.3.2. The overview SEM images can be found in the Appendix. As observed previously, when the concentration of NaCl increase, the particles show well defined crystal faces and the particle size increases. While with addition of the same amount of $CaCl_2$, the particles become even bigger and show more crystalline faces. Some of the particles also show hexagonal morphologies.

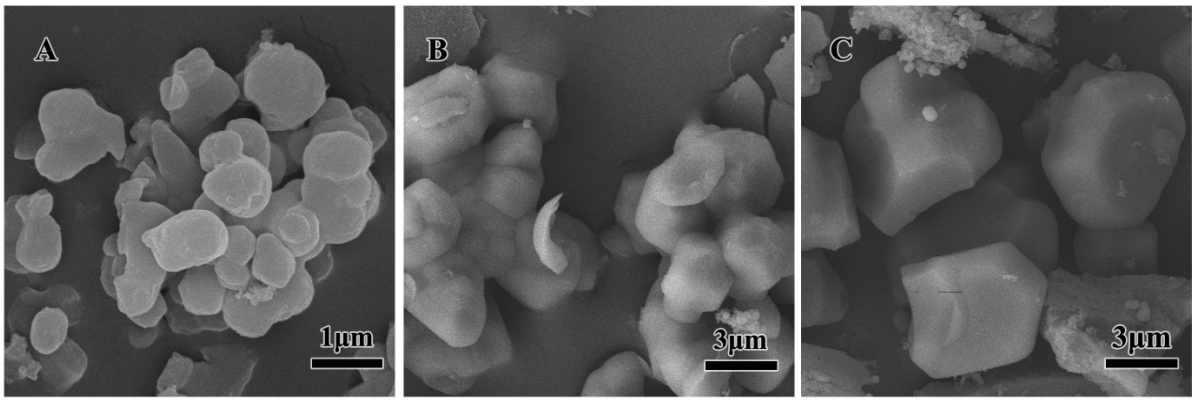

Figure 3.3.2, SEM images of the as-made CFMSs by using $C_{18\text{-}3\text{-}1}$ as template and with addition of NaCl (or $CaCl_2$). The salt molar ratios to $C_{18\text{-}3\text{-}1}$ are (A) 0.0, (B) $NaCl/C_{18\text{-}3\text{-}1}$ =2.0 and (C) $CaCl_2/C_{18\text{-}3\text{-}1}$=2.0.

3.3.2 Hydrochloric acid molar ratio of 1.4 to $C_{18\text{-}3\text{-}1}$

The SAXD patterns of the as-made mesoporous silicas synthesized using different $CaCl_2/C_{18\text{-}3\text{-}1}$ molar ratios when the HCl molar ratio to $C_{18\text{-}3\text{-}1}$ was 1.4 are shown in Figure 3.3.3. Since the amount of CES was different, although the HCl concentration increased, the SAXD patterns remain similar as the results when $HCl/C_{18\text{-}3\text{-}1}$=1.2 with addition of $CaCl_2$. The structures of these samples are supposed to be the $Fm\bar{3}m$ structures (mixed with the $P6_3/mmc$ structures).

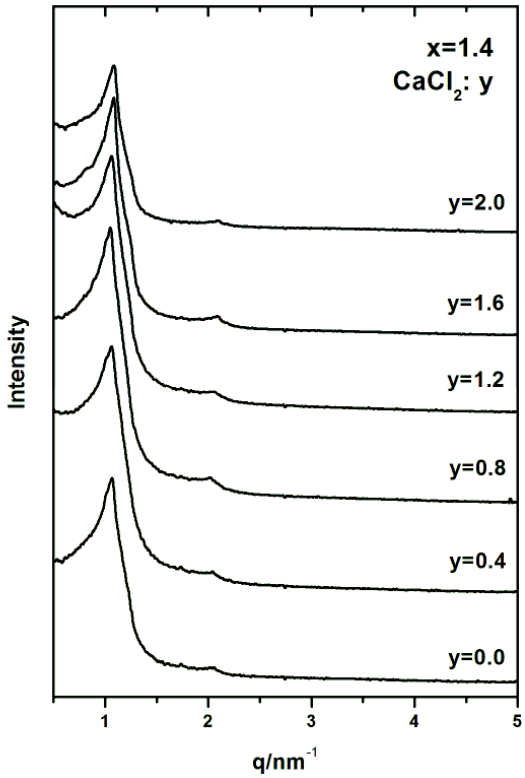

Figure 3.3.3, XRD pattern of the as-made CFMSs by using $C_{18\text{-}3\text{-}1}$ as template and with addition of $CaCl_2$. The reaction molar composition was $C_{18\text{-}3\text{-}1}$: CES: HCl: $CaCl_2$: TEOS: H2O = 1:2: x: y: 15: 2000, where x= 1.6, y= 0.0~2.0.

SEM images with $CaCl_2$ molar ratios of 0.0 and 2.0 to $C_{18\text{-}3\text{-}1}$ are shown in Figure 3.3.4. As the $CaCl_2$ concentration increase, the morphologies achieve a change from roundish to hexagonal, and the particle sizes get bigger. These phenomena are equivalent with the previous results.

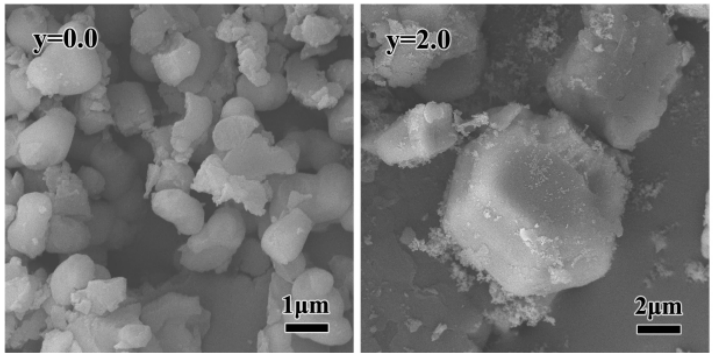

Figure 3.3.5, SEM images of the as-made CFMSs by using $C_{18\text{-}3\text{-}1}$ as template and with addition of $CaCl_2$. The reaction molar composition was $C_{18\text{-}3\text{-}1}$: CES: HCl: $CaCl_2$: TEOS: H_2O = 1: 2: x: y: 15: 2000, where x=1.4, y=0.0 and 2.0.

3.3.3 Hydrochloric acid molar ratio of 1.6 to $C_{18\text{-}3\text{-}1}$

The samples with the HCl molar ratio of 1.6 to $C_{18\text{-}3\text{-}1}$ show interesting SAXD patterns. Another structure transformation has probably been attained. The SAXD patterns of the as-made samples synthesized using different $CaCl_2$ molar ratios to $C_{18\text{-}3\text{-}1}$ are shown in Figure 3.3.6.

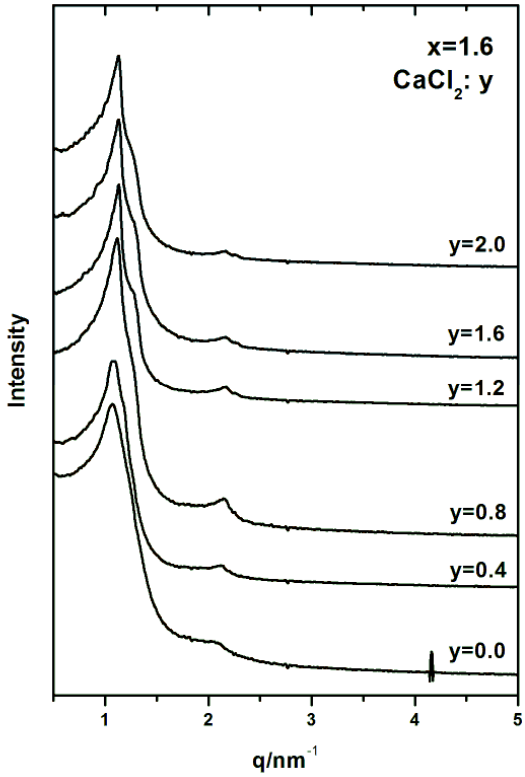

Figure 3.3.6, XRD pattern of the as-made CFMSs by using $C_{18\text{-}3\text{-}1}$ as template and with addition of $CaCl_2$. The reaction molar composition was $C_{18\text{-}3\text{-}1}$: CES: HCl: $CaCl_2$: TEOS: H2O = 1:2: x: y: 15: 2000, where x= 1.6, y= 0.0~2.0.

A further study of the structures suggested from the peaks of the SAXD pattern has been show in Figure 3.3.7, the peak indexed with Miller Indices for the samples with $CaCl_2/C_{18\text{-}3\text{-}1}$ molar ratios of 0.0 and 2.0.

Both of the samples show the peaks from the $Fm\bar{3}m$ structure. But, when $CaCl_2/C_{18\text{-}3\text{-}1}$=0.0, the peaks of the SAXD pattern is very wide, the 200 peak is hid and the 220 and 311 peak are not clear. So this sample possibly has an intergrowth structure. Whereas, the sample with the $CaCl_2/C_{18\text{-}3\text{-}1}$ ratio of 2.0 shows very clear SAXD pattern suggested to have the $Fm\bar{3}m$ structure. It could be a structure transformation from the intergrowth structure to the $Fm\bar{3}m$ structure with increasing of the amounts of $CaCl_2$.

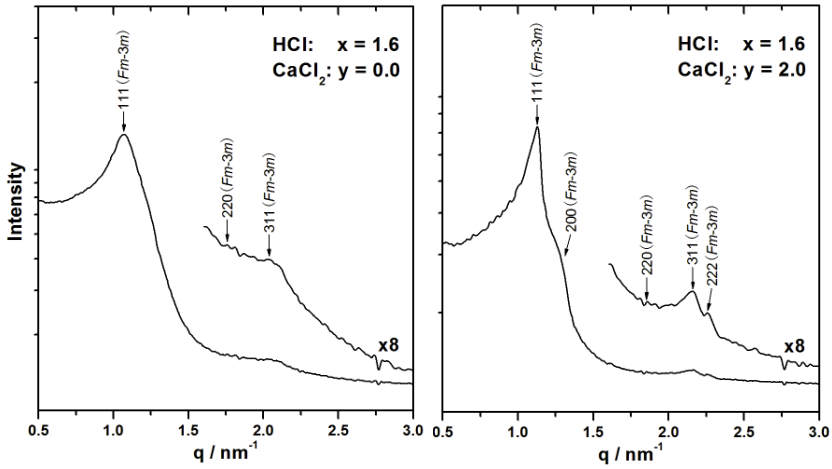

Figure 3.3.6, The peak indexed with Miller Indices of different structures for the samples with $HCl/C_{18\text{-}3\text{-}1}$ molar ratio of 1.6, and $CaCl_2/C_{18\text{-}3\text{-}1}$ molar ratios of 0.0 and 2.0.

Figure 3.3.7 shows the SEM images with high magnifications of the as-made CFMS samples that synthesized when $CaCl_2/C_{18\text{-}3\text{-}1}$=0.0, 0.8 and 1.0. The SEM results show a morphological transformation from roundish to hexagonal crystals. Well defined hexagonal particles are found from the sample with $CaCl_2/C_{18\text{-}3\text{-}1}$ molar ratio of 2.0, indicating that this sample contains much purer $Fm\bar{3}m$ structure than the samples with lower $CaCl_2$ concentration.

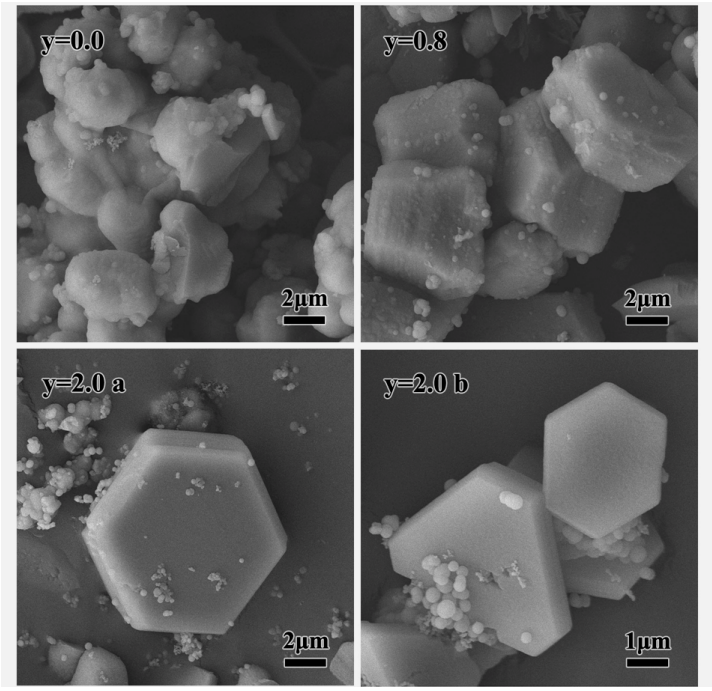

Figure 3.3.8, SEM images of the as-made CFMSs by using $C_{18\text{-}3\text{-}1}$ as template and with addition of $CaCl_2$. The reaction molar composition was $C_{18\text{-}3\text{-}1}$: CES: HCl: $CaCl_2$: TEOS: H_2O = 1: 2: x: y: 15: 2000, where x=1.6, y=0.0, 0.8 and 2.0.

3.3.4 Summary

The structure and the morphology influence have also been obtained when adding $CaCl_2$ into the synthesis system of CFMSs. When $HCl/C_{18\text{-}3\text{-}1}$=1.6, and as the concentration of $CaCl_2$ increased, a structure change from a less well defined $Fm\bar{3}m$ structure to a $Fm\bar{3}m$ structure showing several Bragg peaks has been observed. The latter sample shows well defined hexagonal morphology.

Comparing the different influence between NaCl and $CaCl_2$ for the samples with $HCl/C_{18\text{-}3\text{-}1}$ molar ratio of 1.2, the structures and the morphologies are similar for the samples with the same amounts of NaCl and $CaCl_2$. But the crystallinity and particle size influence of $CaCl_2$ is bigger than NaCl.

4. Conclusion

Salt can influence the structure, the morphology and the particle size to the CFMSs synthesized using $C_{18\text{-}3\text{-}1}$ as template and CES as CSDA. The structure transformation with increasing salt concentration could be attained at a limited range of the added amount of HCl. The morphological changes were consistent with the structures of the samples and observed for the entire pH range. The particle size increased when increasing the concentration of salt in the synthesis system.

The salt influence of NaCl and $CaCl_2$ showed qualitatively similar but quantitatively different effects. The structures and the morphologies are similar for the samples with the same amounts of NaCl and $CaCl_2$, and HCl, while the particle size influence of $CaCl_2$ is bigger than NaCl. Moreover, well defined morphologies could be achieved in a high salt concentration synthesis system, instead of a high acid concentration system.

5. References

(1) Che, S.; Garcia-Bennett, A. E.; Yokoi, T.; Sakamoto, K.; Kunieda, H.; Terasaki, O.; Tatsumi, T. *Nature Materials* **2003**, *2*, 801-805.

(2) Han, L.; Sakamoto, Y.; Terasaki, O.; Li, Y.; Che, S. *Journal of Materials Chemistry* **2007**, *17*, 1216-1221.

(3) Rouquerol, J.; Avnir, D.; Fairbridge, C. W.; Everett, D. H.; Haynes, J. H.; Pernicone, N.; Ramsay, J. D. F.; Sing, K. S. W.; Unger, K. K. *Pure and Applied Chemistry* **1994**, *66*, 1739-1758.

(4) Yanagisawa, T.; Shimizu, T.; Kuroda, K.; Kato, C. *Bulletin of the Chemical Society of Japan* **1990**, *63*, 988-992.

(5) Beck, J. S.; Vartuli, J. C.; Roth, W. J.; Leonowicz, M. E.; Kresge, C. T.; Schmitt, K. D.; Chu, C. T. W.; Olson, D. H.; Sheppard, E. W.; McCullen, S. B.; Higgins, J. B.; Schlenker, J. L. *Journal of the American Chemical Society* **1992**, *114*, 10834-10843.

(6) Kresge, C. T.; Leonowicz, M. E.; Roth, W. J.; Vartuli, J. C.; Beck, J. S. *Nature* **1992**, *359*, 710-712.

(7) Wikimedia; http://en.wikipedia.org/wiki/Lyotropic_liquid_crystal.

(8) Zhao, D. Y.; Huo, Q. S.; Feng, J. L.; Chmelka, B. F.; Stucky, G. D. *Journal of the American Chemical Society* **1998**, *120*, 6024-6036.

(9) Zhao, D. Y.; Feng, J. L.; Huo, Q. S.; Melosh, N.; Fredrickson, G. H.; Chmelka, B. F.; Stucky, G. D. *Science* **1998**, *279*, 548-552.

(10) Huo, Q. S.; Margolese, D. I.; Ciesla, U.; Demuth, D. G.; Feng, P. Y.; Gier, T. E.; Sieger, P.; Firouzi, A.; Chmelka, B. F.; Schuth, F.; Stucky, G. D. *Chemistry of Materials* **1994**, *6*, 1176-1191.

(11) Han, L. Dorctoral Thesis in Chemistry, Stockholm University, Sweden, 2010, 6.

(12) Soler-illia, G. J. D.; Sanchez, C.; Lebeau, B.; Patarin, J. *Chemical Reviews* **2002**, *102*, 4093-4138.

(13) Gao, C.; Qiu, H.; Zeng, W.; Sakamoto, Y.; Terasaki, O.; Sakamoto, K.; Chen, Q.; Che, S. *Chemistry of Materials* **2006**, *18*, 3904-3914.

(14) Gao, C.; Sakamoto, Y.; Terasaki, O.; Sakamoto, K.; Che, S. *Journal of Materials Chemistry* **2007**, *17*, 3591-3602.

(15) Garcia-Bennett, A. E.; Kupferschmidt, N.; Sakamoto, Y.; Che, S.; Terasaki, O. *Angewandte Chemie-International Edition* **2005**, *44*, 5317-5322.

(16) Garcia-Bennett, A. E.; Terasaki, O.; Che, S.; Tatsumi, T. *Chemistry of Materials* **2004**, *16*, 813-821.

(17) Israelachvili, J. N.; Mitchell, D. J.; Ninham, B. W. *Journal of the Chemical Society-Faraday Transactions Ii* **1976**, *72*, 1525-1568.

(18) Huo, Q. S.; Margolese, D. I.; Stucky, G. D. *Chemistry of Materials* **1996**, *8*, 1147-1160.

(19) Han, Y.; Zhang, D.; Chng, L. L.; Sun, J.; Zhao, L.; Zou, X.; Ying, J. Y. *Nature Chemistry* **2009**, *1*, 123-127.

(20) Qiu, H. B.; Xie, J. J.; Che, S. N. *Chemical Communications* **2011**, *47*, 2607-2609.

(21) Zhao, D. Y.; Huo, Q. S.; Feng, J. L.; Kim, J. M.; Han, Y. J.; Stucky, G. D. *Chemistry of Materials* **1999**, *11*, 2668-2672.

(22) Qiu, H.; Sakamoto, Y.; Terasaki, O.; Che, S. *Advanced Materials* **2008**, *20*, 425-+.

(23) Jin, C.; Han, L.; Che, S. *Angewandte Chemie-International Edition* **2009**, *48*, 9268-9272.

(24) Han, L.; Sakamoto, Y.; Che, S. N.; Terasaki, O. *Chemistry-a European Journal* **2009**, *15*, 2818-2825.

(25) Irwin, G. *AccessScience* **2008**, *©McGraw-Hill Companies*, http://www.accessscience.com.

(26) Sakamoto, Y.; Diaz, I.; Terasaki, O.; Zhao, D. Y.; Perez-Pariente, J.; Kim, J. M.; Stucky, G. D. *Journal of Physical Chemistry B* **2002**, *106*, 3118-3123.

(27) Sakamoto, Y.; Han, L.; Che, S.; Terasaki, O. *Chemistry of Materials* **2009**, *21*, 223-229.

(28) Iler, R. K. *The Chemistry of Silica*: Wiley, New York, 1979.

(29) Goldstein, J.; Newbury, D.; Joy, D.; Lyman, C.; Echlin, P.; Lifshin, E.; Sawyer, L.; Michael, J. *Scanning electron mictroscopy and x-ray microanalysis*; 3rd ed.; Kluwer Academic/Plenum, cop.: New York, 2003.

(30) Sing, K. S. W.; Everett, D. H.; Haul, R. A. W.; Moscou, L.; Pierotti, R. A.; Rouquerol, J.; Siemieniewska, T. *Pure and Applied Chemistry* **1985**, *57*, 603-619.

(31) Williams, D. B.; Carter, C. B. *The Transmission Electron Microscope: A Textbook for Materials Science*; Springer Science: New York, 1996, 2009.

(32) Smart, L. E.; Moore, E. A. *Solid State Chemistry: An Introductuion*; 3rd ed.; CRC Press: U.S., 2005.

(33) Huo, Q.; Margolese, D. I.; Strucky, G. D. *Chem. Mater*. **1996**, *8*, 1147-1160.

(34) Kleitz, F.; Liu, D. N.; Anilkumar, G. M.; Park, I. S.; Solovyov, L. A.; Shmakov, A. N.; Ryoo, R. *Journal of Physical Chemistry B* **2003**, *107*, 14296-14300.

Acknowledgments

This is the small personal part in this thesis. So this section will be written in Chin-English. During the one and a half years stay in Sweden, I learnt a lot not only about research, but also about life.

Dear Viveka, all the discussions we had meant a lot to me. You always gave me very nice suggestions and showed me the right way I need to go, and made me feel safe. I think I have the talent to make people crazy, but you were never angry with me or complained. Thank you for all the patience and for taking care of me. It was my fortune and pleasure to have a supervisor as nice as you.

Dear Prof. Che, although we didn't get many chances to discuss, you've provided me with very good ideas. Thank you for your good suggestions and greeting. Also, the skills I learnt from your group before I came to Sweden, helped me do good work here in Lund. I miss you a lot when I'm here in Sweden.

Lu Han, thank you for the long distance chatting discussions. Since the work in this thesis is followed by your previous work, your suggestion and explanation helped a lot to me.

Sweet Emelie, I always ask you a lot of questions and even bother you with SMS during holidays, but you never complained and described to me or discussed with me very patiently, thank you so much. Also thank you for the super useful help with my thesis writing.

Tomas and Gunnel, thank you for helping me take very nice SEM images. Also thanks to Segad for the kind help with the SAXS instrument.

Dear irmã Alexandra, it is very sad that I could not have you here during the busiest time of the work of my master thesis. But you were one of the main parts of my life here, during the one and a half years in Lund. Thank you for all the company during work, talks, lunches and so on. You shared all my complaints, watched me cry and cheered for my happiness. Thank you for all the time spent with you here in Lund.

Amazing Saskia and my lively neighbor Xuan Zhang, thank you for the food you prepared for me during my desperate writing time. It was so nice of you to cook for me so that I survived during the busiest time. Also thanks to Johanna for all the delicious desserts. Your food made me happy and made me work energetically.

Debby, Divya and all the friends from the department of Physical Chemistry, I was always walking around to ask for your help and complained to you about everything in my life. I became more independent within these one and a half years because of what you guys taught me and you took care of me very well. Thank you for all your encouragements and patience. I also enjoyed all the after-works we had.

All my Chinese friends, not only the Chinese friends here in Lund but also from China, thank you for your kind care and encouragement. Especially to Mona, I'm lucky to meet such a nice sister as you here in Lund. We had quite a lot of happy times together. Thank you for everything.

Dear Jian (my "someone"), Sweden is a magic place that made me get to know you during my master study. Fortunately, we can work in very close cities soon. Thank you for understanding me all the time, and also for your cheering.

My dear parents, you are the ones I want to thank the most. You support me living in Sweden, taught me how to cook through Skype, shared my happiness and complaints. Although I'm far from home now, my heart is always close to you.

From,

Ruiyu Lin (Jessie)

林芮羽

Appendix

1. Synthesis of CFMSs Synthesized with C18-3-1

1.1 Composition of the samples

The molar ratios are $C_{18\text{-}3\text{-}1}$:2CES: xHCl: 15TEOS:2000H_2O, x=0.8~1.8.

No.	HCl x	Ionic Strength	pH		Supposed Structure	Lattice spacing for different structures	Mophology
			Before[1]	After[2]			
1	0.8	0.1450	1.62	8.67	*Fm*$\bar{3}$*m* *P*6$_3$/*mmc*	a=10.06 nm for *Fm*$\bar{3}$*m* a'=7.41 nm, c'=12.04 nm for *P*6$_3$/*mmc*	roundish
2	1.0	0.1500	1.58	8.68	*Fm*$\bar{3}$*m* *P*6$_3$/*mmc*	a=10.69 nm for *Fm*$\bar{3}$*m*	roundish
3	1.2	0.1550	1.56	8.66	*Fm*$\bar{3}$*m* *P*6$_3$/*mmc*	a=9.94 nm for *Fm*$\bar{3}$*m* a'=7.48 nm, c'=12.15 nm for *P*6$_3$/*mmc*	roundish
4	1.4	0.1600	1.49	7.93	*Fm*$\bar{3}$*m* *P*6$_3$/*mmc* *Fd*$\bar{3}$*m*	a=9.90 nm for *Fm*$\bar{3}$*m*	roundish layered
5	1.6	0.1650	1.29	5.95	*Fd*$\bar{3}$*m*	a''=17.37 nm for *Fd*$\bar{3}$*m*	layered hexagonal
6	1.7	0.1675	1.24	5.56	*Fd*$\bar{3}$*m*	a''=17.12 nm for *Fd*$\bar{3}$*m*	hexagonal cubic
7	1.8	0.1700	1.18	5.18	*Fd*$\bar{3}$*m*	a''=17.13 nm for *Fd*$\bar{3}$*m*	hexagonal cubic

1. Before adding CES and TEOS to begin the reaction, the solution only contains $C_{18\text{-}3\text{-}1}$, HCl and water.
2. After the 2 hours reaction when stopping stirring.

1.2 SAXD measurements

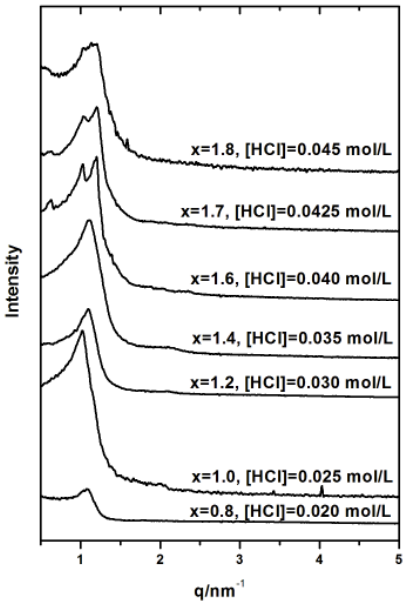

1.3 Morphologies

HCl concentration	SEM (overview)	SEM (high magnification)	
x=0.8 [HCl]=0.020 mol/L	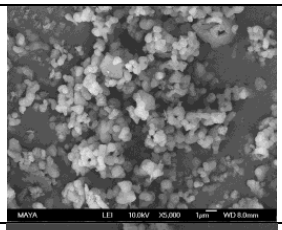	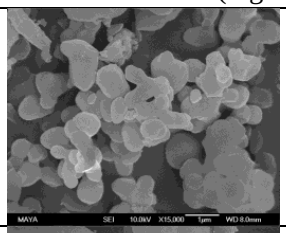	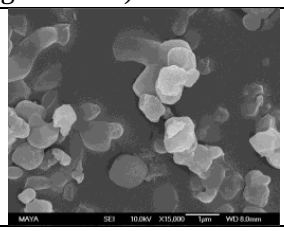
x=1.0 [HCl]=0.025 mol/L	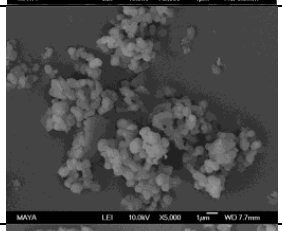	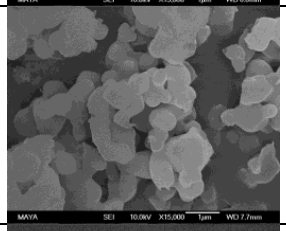	
x=1.2 [HCl]=0.030 mol/L	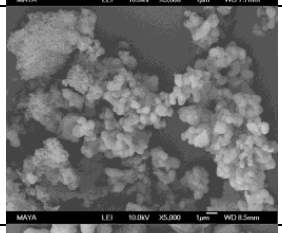	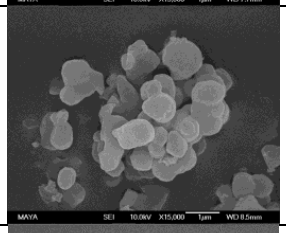	
x=1.4 [HCl]=0.035 mol/L	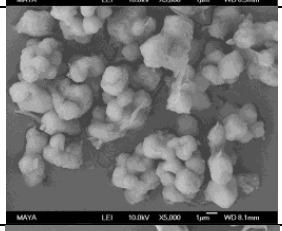	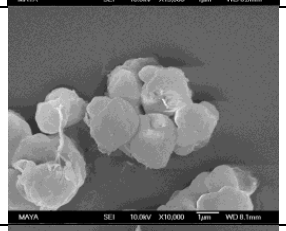	
x=1.6 [HCl]=0.040 mol/L	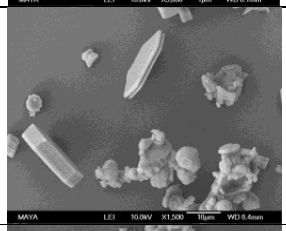	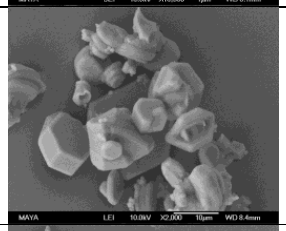	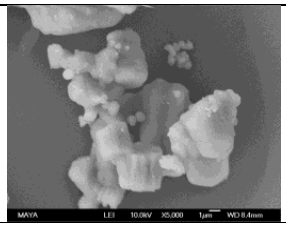
x=1.7 [HCl]=0.0425 mol/L	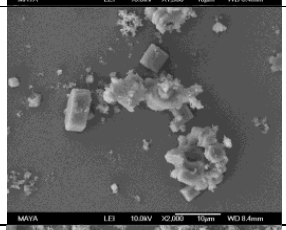	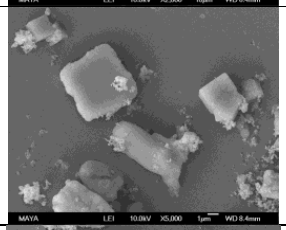	
x=1.8 [HCl]=0.045 mol/L	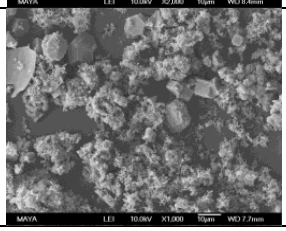	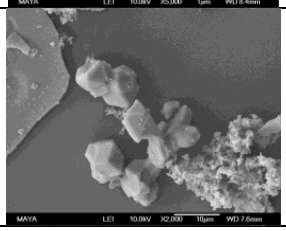	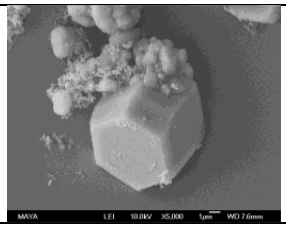

2. Influence of sodium chloride

2.1 Hydrochloric acid concentration of 0.025 mol/L, molar ratio of 1.0 to $C_{18\text{-}3\text{-}1}$

Composition of the samples

The molar ratios are $C_{18\text{-}3\text{-}1}$:2CES: xHCl: yNaCl: 15TEOS:2000H_2O, x=1.0, y=0.0~0.8.

No.	NaCl y	Ionic Strength	pH		Supposed Structure	Lattice spacing for different structures	Morphology
			Before[1]	After[2]			
1	0.0	0.1500	1.58	8.68	$Fm\bar{3}m$ $P6_3/mmc$	a=10.69 nm for $Fm\bar{3}m$	roundish
2	0.2	0.1550	--	--	$Fm\bar{3}m$ $P6_3/mmc$	a=10.19 nm for $Fm\bar{3}m$	--
3	0.4	0.1600	--	--	$Fm\bar{3}m$ $P6_3/mmc$	a=10.20 nm for $Fm\bar{3}m$	--
4	0.6	0.1650	--	--	$Fm\bar{3}m$ $P6_3/mmc$	a=10.37 nm for $Fm\bar{3}m$	--
5	0.8	0.1700	--	--	$Fm\bar{3}m$ $P6_3/mmc$	a=10.27 nm for $Fm\bar{3}m$	roundish

1. Before adding CES and TEOS to begin the reaction, the solution only contains $C_{18\text{-}3\text{-}1}$, HCl, NaCl, H_2O.
2. After the 2 hours reaction when stopping stirring.

SAXD measurements

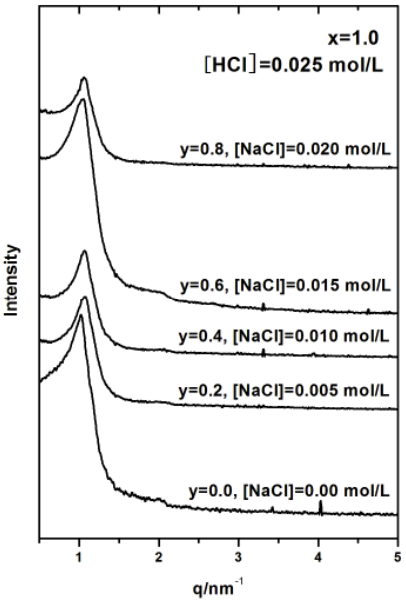

Morphologies

NaCl concentration	SEM (overview)	SEM (high magnification)
y=0.0 [NaCl] =0.00 mol/L	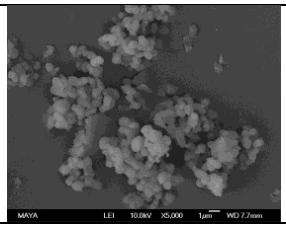	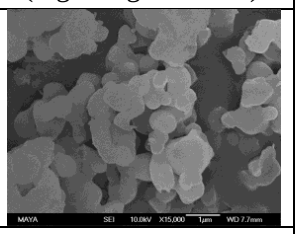
y=0.2 [NaCl] =0.005 mol/L	--	--
y=0.4 [NaCl] =0.010 mol/L	--	--
y=0.6 [NaCl] =0.015 mol/L	--	--
y=0.8 [NaCl] =0.020 mol/L	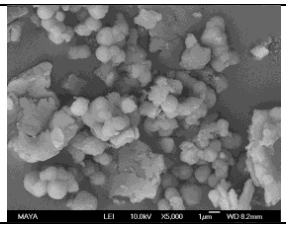	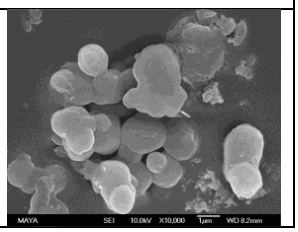

2.2 Hydrochloric acid concentration of 0.030 mol/L, molar ratio of 1.2 to $C_{18\text{-}3\text{-}1}$

Composition of the samples

The molar ratios are $C_{18\text{-}3\text{-}1}$:2CES: xHCl: yNaCl: 15TEOS:2000H_2O, x=1.2, y=0.0~2.0.

No.	NaCl y	Ionic Strength	pH		Supposed Structure	Lattice spacing for different structures	Morphology
			Before[1]	After[2]			
1	0.0	0.1550	1.56	8.84	*Fm*$\bar{3}$*m* *P*6$_3$/*mmc*	a=9.95 nm for *Fm*$\bar{3}$*m* a'=7.48, c'=12.15 nm for *P*6$_3$/*mmc*	roundish
2	0.4	0.1650	1.57	8.95	*Fm*$\bar{3}$*m* *P*6$_3$/*mmc*	a=10.03 nm for Fm3m a'=7.45, c'=12.11 nm for *P*6$_3$/*mmc*	--
3	0.8	0.1750	1.55	8.96	*Fm*$\bar{3}$*m* *P*6$_3$/*mmc*	a=10.08 nm for *Fm*$\bar{3}$*m* a'=7.11, c'=11.56 nm for *P*6$_3$/*mmc*	roundish
4	1.2	0.1850	1.54	8.89	*Fm*$\bar{3}$*m* *P*6$_3$/*mmc*	a=10.02 nm for *Fm*$\bar{3}$*m* a'=7.51, c'=12.21 nm for *P*6$_3$/*mmc*	--
5	1.6	0.1950	1.55	9.02	*Fm*$\bar{3}$*m* *P*6$_3$/*mmc*	a=10.03 nm for *Fm*$\bar{3}$*m* a'=7.49, c'=12.18 nm for *P*6$_3$/*mmc*	--
6	2.0	0.2050	1.55	8.92	*Fm*$\bar{3}$*m* *P*6$_3$/*mmc*	a=10.05 nm for *Fm*$\bar{3}$*m* a'=7.10, c'=11.60 nm for *P*6$_3$/*mmc*	roundish

1. Before adding CES and TEOS to begin the reaction, the solution only contains $C_{18\text{-}3\text{-}1}$, HCl, NaCl, H_2O.
2. After the 2 hours reaction when stopping stirring.

SAXD measurements

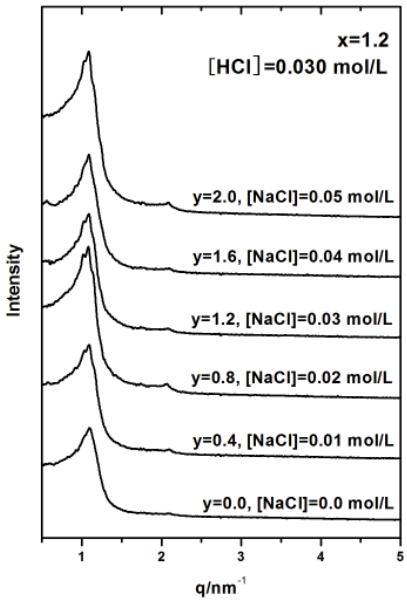

Morphologies

NaCl concentration	SEM (overview)	SEM (magnification)
y=0.0 [NaCl]=0.0 mol/L	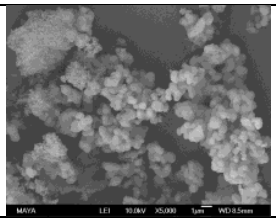	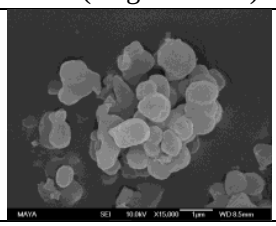
y=0.4 [NaCl]=0.01 mol/L	--	--
y=0.8 [NaCl]=0.02 mol/L	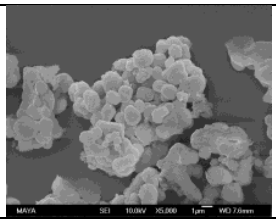	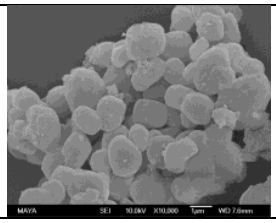
y=1.2 [NaCl]=0.03 mol/L	--	--
y=1.6 [NaCl]=0.04 mol/L	--	--
y=2.0 [NaCl]=0.05 mol/L	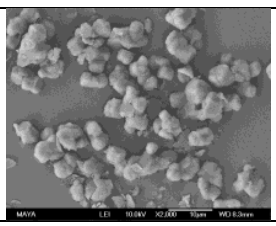	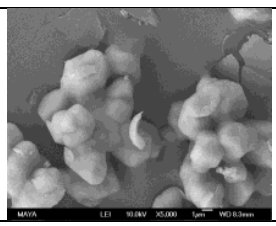

2.3 Hydrochloric acid concentration of 0.035 mol/L, molar ratio of 1.4 to $C_{18\text{-}3\text{-}1}$

Composition of the samples

The molar ratios are $C_{18\text{-}3\text{-}1}$:2CES: xHCl: yNaCl: 15TEOS:2000H_2O, x=1.4, y=0.0~2.0.

No.	NaCl y	Ionic Strength	pH		Supposed Structure	Lattice spacing for different structures	Morphology
			Before[1]	After[2]			
1	0.0	0.1600	1.49	7.93	$Fm\bar{3}m$ $P6_3/mmc$ $Fd\bar{3}m$	a=9.90 nm for $Fm\bar{3}m$	roundish layered
2	0.4	0.1700	1.49	8.28	$Fm\bar{3}m$ $P6_3/mmc$ $Fd\bar{3}m$	a=9.91 nm for $Fm\bar{3}m$	roundish layered
3	0.8	0.1800	1.49	8.12	$Fm\bar{3}m$ $P6_3/mmc$ $Fd\bar{3}m$	a=10.05 nm for $Fm\bar{3}m$	roundish layered
4	1.2	0.1900	1.48	8.22	$Fm\bar{3}m$ $P6_3/mmc$ $Fd\bar{3}m$	a=10.01 nm for $Fm\bar{3}m$	crystalline layered
5	1.6	0.2000	1.52	7.90	$Fm\bar{3}m$ $P6_3/mmc$ $Fd\bar{3}m$	a=10.14 nm for $Fm\bar{3}m$ a'=7.38, c'=11.99 nm for $P6_3/mmc$ a''=17.91 nm for $Fd\bar{3}m$	crystalline layered
6	2.0	0.2100	1.52	7.64	$Fm\bar{3}m$ $P6_3/mmc$ $Fd\bar{3}m$	a=10.29 nm for $Fm\bar{3}m$ a''=17.93 nm for $Fd\bar{3}m$	hexagonal layered

1. Before adding CES and TEOS to begin the reaction, the solution only contains $C_{18\text{-}3\text{-}1}$, HCl, NaCl, H_2O.
2. After the 2 hours reaction when stopping stirring.

SAXD measurements

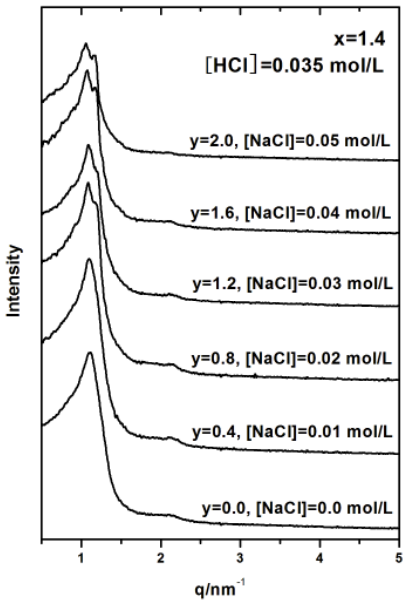

Morphologies

NaCl concentration	SEM (overview)	SEM (high magnification)	
y=0.0 [NaCl]=0.0 mol/L	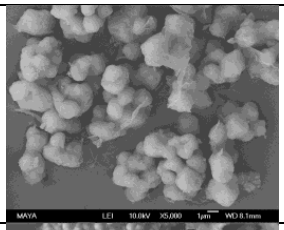	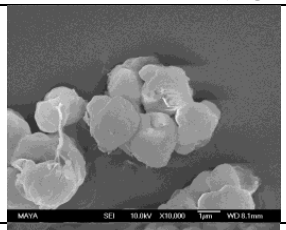	
y=0.4 [NaCl]=0.01 mol/L	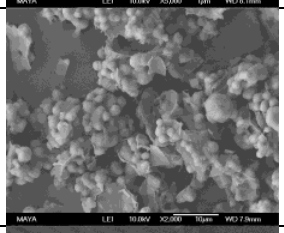	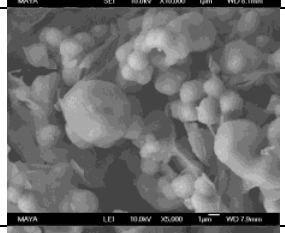	
y=0.8 [NaCl]=0.02 mol/L	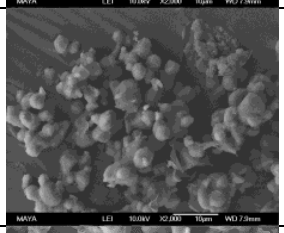	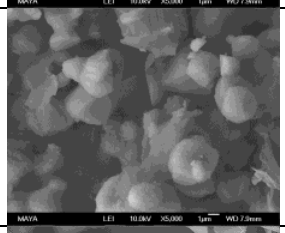	
y=1.2 [NaCl]=0.03 mol/L	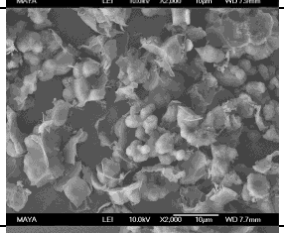	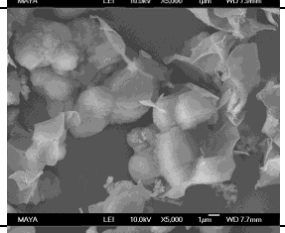	
y=1.6 [NaCl]=0.04 mol/L	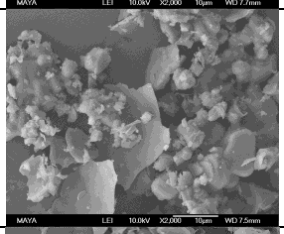	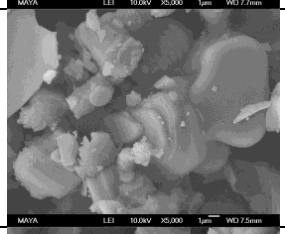	
y=2.0 [NaCl]=0.05 mol/L	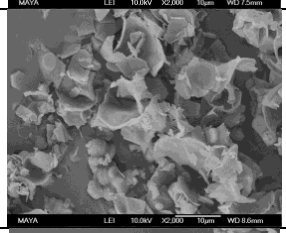 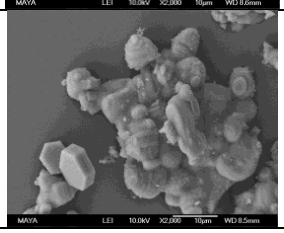	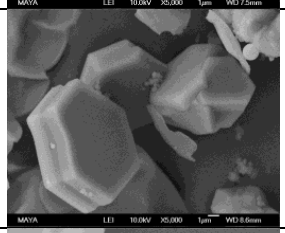 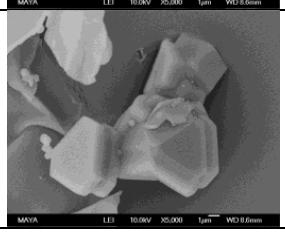	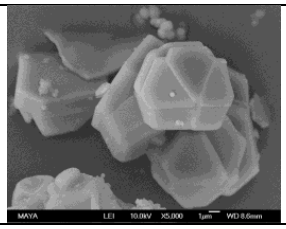

2.4 Hydrochloric acid concentration of 0.035 mol/L, molar ratio of 1.6 to $C_{18\text{-}3\text{-}1}$

Composition of the samples

The molar ratios are $C_{18\text{-}3\text{-}1}$:2CES: xHCl: yNaCl: 15TEOS:2000H_2O, x=1.6, y=0.0~2.0.

No.	NaCl y	Ionic Strength	pH		Supposed Structure	Lattice spacing for different structures	Morphology
			Before[1]	After[2]			
1	0.0	0.1650	1.29	5.95	$Fd\bar{3}m$	a''=17.37 nm for $Fd\bar{3}m$	hexagonal layered
2	0.4	0.1750	1.33	6.06	$Fd\bar{3}m$	a''=17.46 nm for $Fd\bar{3}m$	--
3	0.8	0.1850	1.33	5.92	$Fd\bar{3}m$	a''=17.39 nm for $Fd\bar{3}m$	hexagonal layered cubic
4	1.2	0.1950	1.34	5.97	$Fd\bar{3}m$	a''=17.54 nm for $Fd\bar{3}m$	--
5	1.6	0.2050	1.32	6.13	$Fd\bar{3}m$	a''=17.63 nm for $Fd\bar{3}m$	--
6	2.0	0.2150	1.32	6.02	$Fd\bar{3}m$	a''=17.54 nm for $Fd\bar{3}m$	hexagonal layered cubic

1. Before adding CES and TEOS to begin the reaction, the solution only contains $C_{18\text{-}3\text{-}1}$, HCl, NaCl, H_2O.
2. After the 2 hours reaction when stopping stirring.

SAXD measurements

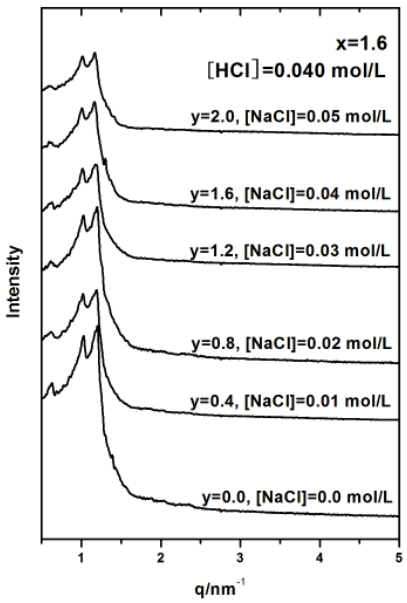

Morphologies

NaCl concentration	SEM (overview)	SEM (high magnification)	
y=0.0 [NaCl]=0.0 mol/L	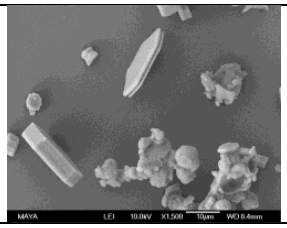	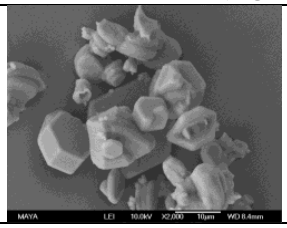	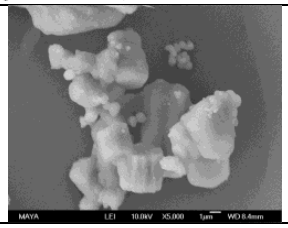
y=0.4 [NaCl]=0.01 mol/L	--	--	
y=0.8 [NaCl]=0.02 mol/L	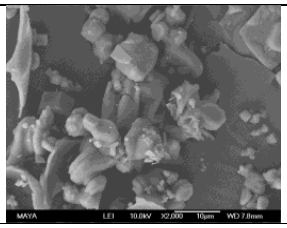	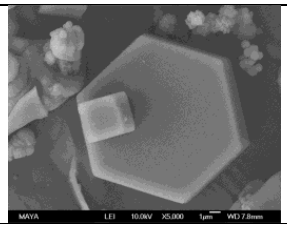	
y=1.2 [NaCl]=0.03 mol/L	--	--	
y=1.6 [NaCl]=0.04 mol/L	--	--	
y=2.0 [NaCl]=0.05 mol/L	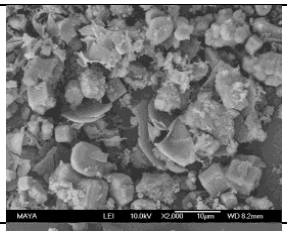 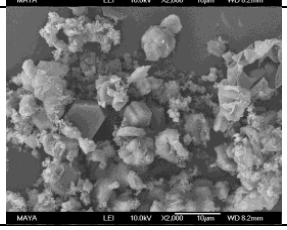	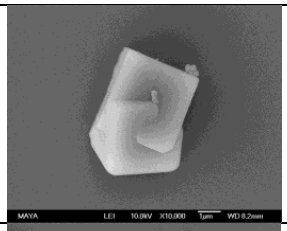 	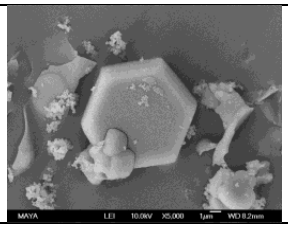

2.5 Hydrochloric acid concentration of 0.0425 mol/L, molar ratio of 1.7 to $C_{18\text{-}3\text{-}1}$

Composition of the samples

The molar ratios are $C_{18\text{-}3\text{-}1}$:2CES: xHCl: yNaCl: 15TEOS:2000H_2O, x=1.7, y=0.0~0.8.

No.	NaCl y	Ionic Strength	pH		Supposed Structure	Lattice spacing for different structures	Morphology
			Before[1]	After[2]			
1	0.0	0.1675	1.24	5.56	$Fd\bar{3}m$	a''=17.14 nm for $Fd\bar{3}m$	hexagonal, cubic
2	0.2	0.1725	--	--	$Fd\bar{3}m$	a''=17.07 nm for $Fd\bar{3}m$	--
3	0.4	0.1775	--	--	$Fd\bar{3}m$	a''=17.34 nm for $Fd\bar{3}m$	--
4	0.6	0.1825	--	--	$Fd\bar{3}m$	a''=17.13 nm for $Fd\bar{3}m$	--
5	0.8	0.1875	--	--	$Fd\bar{3}m$	a''=17.38 nm for $Fd\bar{3}m$	hexagonal, cubic

1. Before adding CES and TEOS to begin the reaction, the solution only contains $C_{18\text{-}3\text{-}1}$, HCl, NaCl, H_2O.
2. After the 2 hours reaction when stopping stirring.

SAXD measurements

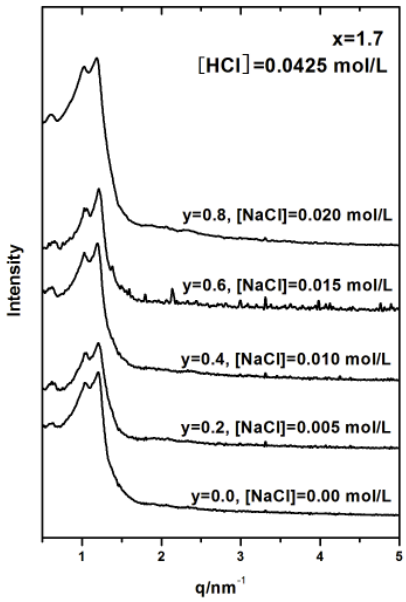

Morphologies

NaCl concentration	SEM (overview)	SEM (high magnification)
y=0.0 [NaCl]=0.00 mol/L	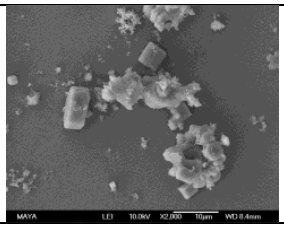	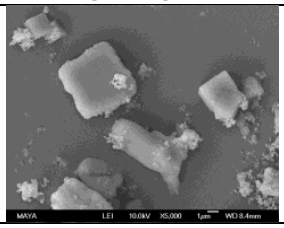
y=0.2 [NaCl]=0.005 mol/L	--	--
y=0.4 [NaCl]=0.010 mol/L	--	--
y=0.6 [NaCl]=0.015 mol/L	--	--
y=0.8 [NaCl]=0.020 mol/L	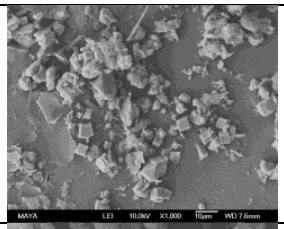	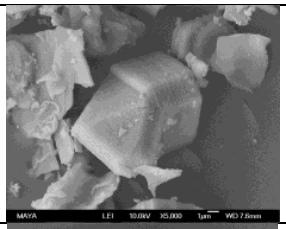
	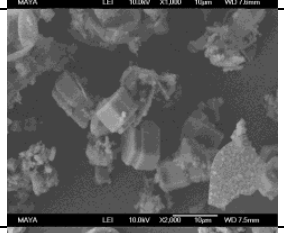	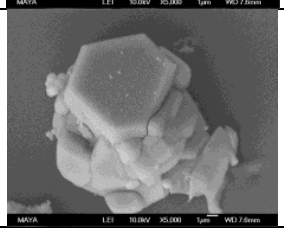
	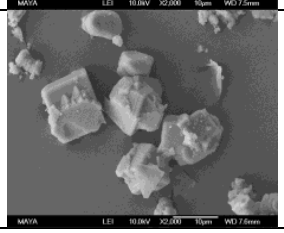	

3. Influence of calcium chloride

3.1 Hydrochloric acid concentration of 0.030 mol/L, molar ratio of 1.2 to $C_{18\text{-}3\text{-}1}$

Composition of the samples

The molar ratios are $C_{18\text{-}3\text{-}1}$:2CES: xHCl: y$CaCl_2$: 15TEOS:2000H_2O, x=1.2, y=0.0~2.0.

No.	$CaCl_2$ y	Ionic Strength	pH		Supposed Structure	Lattice spacing for different structures	Morphology
			Before[1]	After[2]			
1	0.0	0.1550	1.56	8.84	*Fm*$\bar{3}$*m* *P*6$_3$/*mmc*	a=10.08 nm for *Fm*$\bar{3}$*m* a'=7.16, c'=11.64 nm for *P*6$_3$/*mmc*	roundish
2	0.4	0.1850	1.55	8.91	*Fm*$\bar{3}$*m* *P*6$_3$/*mmc*	a=10.15 nm for Fm3m a'=7.57, c'=12.30 nm for *P*6$_3$/*mmc*	--
3	0.8	0.2150	1.55	8.99	*Fm*$\bar{3}$*m* *P*6$_3$/*mmc*	a=10.14 nm for *Fm*$\bar{3}$*m* a'=7.46, c'=12.12 nm for *P*6$_3$/*mmc*	--
4	1.2	0.2450	1.54	9.02	*Fm*$\bar{3}$*m* *P*6$_3$/*mmc*	a=10.28 nm for *Fm*$\bar{3}$*m* a'=7.61, c'=12.38 nm for *P*6$_3$/*mmc*	--
5	1.6	0.2750	1.53	9.02	*Fm*$\bar{3}$*m* *P*6$_3$/*mmc*	a=10.22 nm for *Fm*$\bar{3}$*m*	--
6	2.0	0.3050	1.53	9.00	*Fm*$\bar{3}$*m* *P*6$_3$/*mmc*	a=10.45 nm for *Fm*$\bar{3}$*m* a'=7.17, c'=11.65 nm for *P*6$_3$/*mmc*	crystalline layered

1. Before adding CES and TEOS to begin the reaction, the solution only contains $C_{18\text{-}3\text{-}1}$, HCl, $CaCl_2$, H_2O.
2. After the 2 hours reaction when stopping stirring.

SAXD measurements

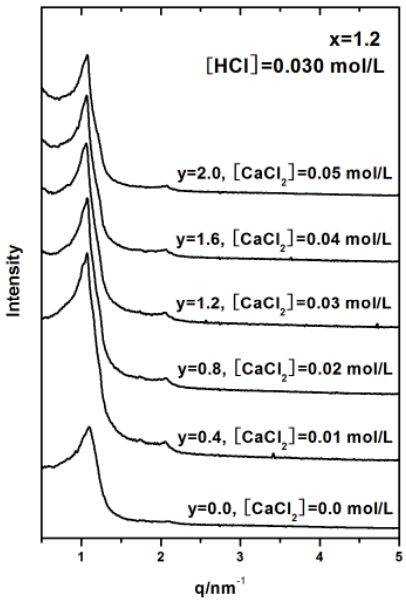

Morphologies

$CaCl_2$ concentration	SEM (overview)	SEM (high magnification)
y=0.0 $[CaCl_2]$=0.0 mol/L	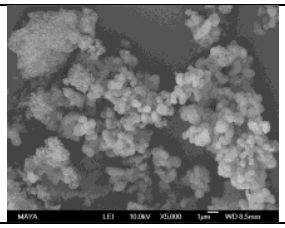	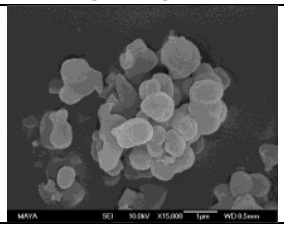
y=0.4 $[CaCl_2]$=0.01 mol/L	--	--
y=0.8 $[CaCl_2]$=0.02 mol/L	--	--
y=1.2 $[CaCl_2]$=0.03 mol/L	--	--
y=1.6 $[CaCl_2]$=0.04 mol/L	--	--
y=2.0 $[CaCl_2]$=0.05 mol/L	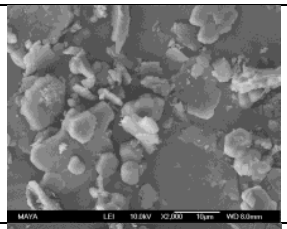 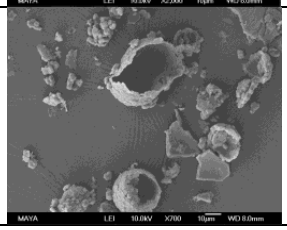	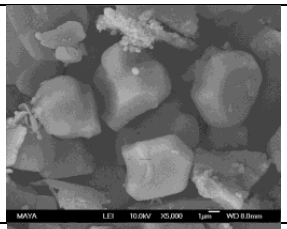 

3.2 Hydrochloric acid concentration of 0.035 mol/L, molar ratio of 1.4 to $C_{18\text{-}3\text{-}1}$

Composition of the samples

The molar ratios are $C_{18\text{-}3\text{-}1}$:2CES: xHCl: y$CaCl_2$: 15TEOS:2000H_2O, x=1.4, y=0.0~2.0.

No.	$CaCl_2$ y	Ionic Strength	pH		Supposed Structure	Lattice spacing for different structures	Morphology
			Before[1]	After[2]			
1	0.0	0.1600	1.50	8.78	*Fm*$\bar{3}$*m* *P*6$_3$/*mmc*	a=10.26 nm for *Fm*$\bar{3}$*m* a'=7.54, c'=12.26 nm for *P*6$_3$/*mmc*	roundish
2	0.4	0.1900	1.48	8.72	*Fm*$\bar{3}$*m* *P*6$_3$/*mmc*	a=10.28 nm for Fm3m a'=7.26, c'=11.87 nm for *P*6$_3$/*mmc*	--
3	0.8	0.2200	1.48	8.72	*Fm*$\bar{3}$*m* *P*6$_3$/*mmc*	a=10.39 nm for *Fm*$\bar{3}$*m* a'=7.67, c'=12.47 nm for *P*6$_3$/*mmc*	--
4	1.2	0.2500	1,46	8.83	*Fm*$\bar{3}$*m* *P*6$_3$/*mmc*	a=10.28 nm for *Fm*$\bar{3}$*m* a'=7.58, c'=12.32 nm for *P*6$_3$/*mmc*	--
5	1.6	0.2800	1.44	8.99	*Fm*$\bar{3}$*m* *P*6$_3$/*mmc*	a=10.09 nm for *Fm*$\bar{3}$*m*	--
6	2.0	0.3100	1.45	8.76	*Fm*$\bar{3}$*m* *P*6$_3$/*mmc*	a=10.05 nm for *Fm*$\bar{3}$*m*	crystalline layered

1. Before adding CES and TEOS to begin the reaction, the solution only contains $C_{18\text{-}3\text{-}1}$, HCl, $CaCl_2$, H_2O.
2. After the 2 hours reaction when stopping stirring.

SAXD measurements

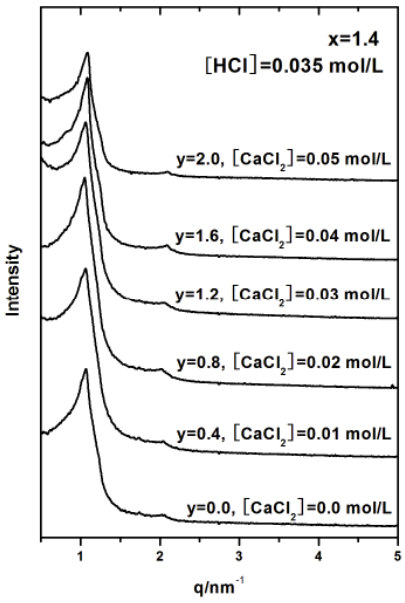

Morphologies

$CaCl_2$ concentration	SEM (overview)	SEM (high magnification)
y=0.0 [$CaCl_2$] =0.0 mol/L	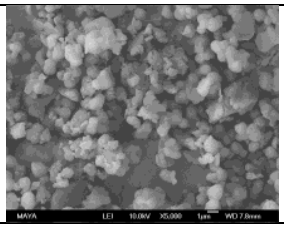	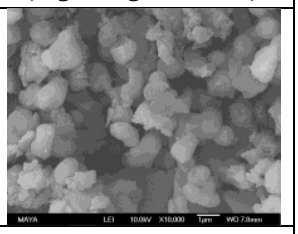
y=0.4 [$CaCl_2$] =0.01 mol/L	--	--
y=0.8 [$CaCl_2$] =0.02 mol/L	--	--
y=1.2 [$CaCl_2$] =0.03 mol/L	--	--
y=1.6 [$CaCl_2$] =0.04 mol/L	--	--
y=2.0 [$CaCl_2$] =0.05 mol/L	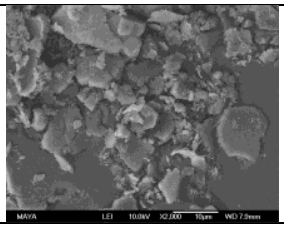	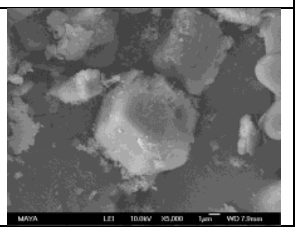

3.3 Hydrochloric acid concentration of 0.040 mol/L, molar ratio of 1.6 to $C_{18\text{-}3\text{-}1}$

Composition of the samples

The molar ratios are $C_{18\text{-}3\text{-}1}$:2CES: xHCl: y$CaCl_2$: 15TEOS:2000H_2O, x=1.6, y=0.0~2.0.

No.	$CaCl_2$ y	Ionic Strength	pH		Supposed Structure	Lattice spacing for different structures	Morphology
			Before[1]	After[2]			
1	0.0	0.1650	1.38	8.81	$Fm\bar{3}m$ $P6_3/mmc$	a=10.19 nm for $Fm\bar{3}m$	crystalline layered
2	0.4	0.1950	1.38	8.58	$Fm\bar{3}m$ $P6_3/mmc$	a=9.96 nm for Fm3m	--
3	0.8	0.2250	1.37	8.70	$Fm\bar{3}m$ $P6_3/mmc$	a=9.61 nm for $Fm\bar{3}m$	crystalline
4	1.2	0.2550	1.36	8.49	$Fm\bar{3}m$ $P6_3/mmc$	a=9.85 nm for $Fm\bar{3}m$	--
5	1.6	0.2850	1.35	8.57	$Fm\bar{3}m$ $P6_3/mmc$	a=9.66 nm for $Fm\bar{3}m$	--
6	2.0	0.3150	1.36	8.68	$Fm\bar{3}m$ $P6_3/mmc$	a=9.66 nm for $Fm\bar{3}m$	hexagonal

1. Before adding CES and TEOS to begin the reaction, the solution only contains $C_{18\text{-}3\text{-}1}$, HCl, $CaCl_2$, H_2O.
2. After the 2 hours reaction when stopping stirring.

SAXD measurements

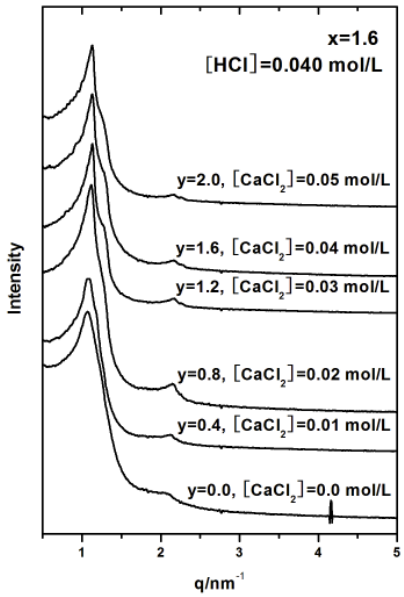

Morphologies

$CaCl_2$ concentration	SEM (overview)	SEM (high magnification)
y=0.0 [$CaCl_2$]=0.0 mol/L	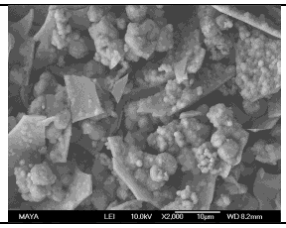	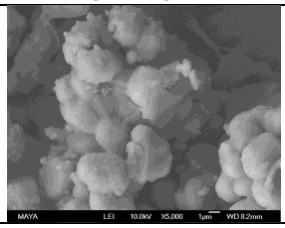
y=0.4 [$CaCl_2$]=0.01 mol/L	--	--
y=0.8 [$CaCl_2$]=0.02 mol/L	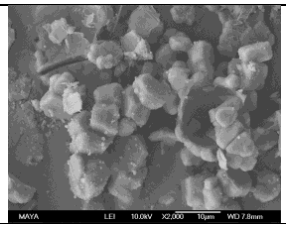	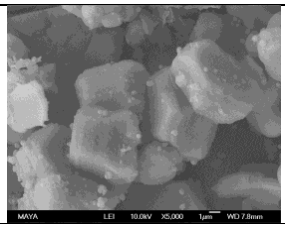
y=1.2 [$CaCl_2$]=0.03 mol/L	--	--
y=1.6 [$CaCl_2$]=0.04 mol/L	--	--
y=2.0 [$CaCl_2$]=0.05 mol/L